Free energy functionals for polarization fluctuations: Pekar factor revisited

Mohammadhasan Dinpajooh,[1] Marshall D. Newton,[2] and Dmitry V. Matyushov*[3]
[1)] *School of Molecular Sciences, Arizona State University, PO Box 871604, Tempe, AZ 85287-1604*
[2)] *Brookhaven National Laboratory, Chemistry Department, Box 5000, Upton, NY 11973-5000, United States*
[3)] *Department of Physics and School of Molecular Sciences, Arizona State University, PO Box 871504, Tempe, AZ 85287-1504* [a)]

The separation of slow nuclear and fast electronic polarization in problems related to electron mobility in polarizable media was considered by Pekar 70 years ago. Within dielectric continuum models, this separation leads to the Pekar factor in the free energy of solvation by the nuclear degrees of freedom. The main qualitative prediction of Pekar's perspective is a significant, by about a factor of two, drop of the nuclear solvation free energy compared to the total (electronic plus nuclear) free energy of solvation. The Pekar factor enters the solvent reorganization energy of electron transfer reactions and is a significant mechanistic parameter accounting for the solvent effect on electron transfer. Here, we study the separation of the fast and slow polarization modes in polar molecular liquids (polarizable dipolar liquids and polarizable water force fields) without relying on the continuum approximation. We derive the nonlocal free energy functional and use atomistic numerical simulations to obtain nonlocal, reciprocal space electronic and nuclear susceptibilities. A consistent transition to the continuum limit is introduced by extrapolating the results of finite-size numerical simulation to zero wavevector. The continuum nuclear susceptibility extracted from simulations is numerically close to the Pekar factor. However, we derive a new functionality involving the static and high-frequency dielectric constants. The main distinction of our approach from the traditional theories is found for the solvation free energy due to the nuclear polarization: the anticipated significant drop of its magnitude with increasing liquid polarizability does not occur. The reorganization energy of electron transfer is either nearly constant with increasing the solvent polarizability and the corresponding high-frequency dielectric constant (polarizable dipolar liquids) or actually noticeably increases (polarizable force fields of water).

I. Introduction

Localized electronic states in polarizable media, such as those of dissolved molecules, are distorted compared to the gas phase due to the medium deformation known as solvation. If the electronic state is isolated (infinite dilution) and the center of localization does not move, the deformation of the medium is associated with the free energy of equilibrium solvation. For conduction electrons, this solvation free energy can dominate the energy gained in delocalizing them (approximately equal to half of the bandwidth[1]) and localized polarons become energetically more stable than conduction plane waves.[2–4]

Charge mobility requires, in addition to statistical considerations, involvement of time scales relevant for the electronic and medium dynamics. In order to appreciate the issues involved, one can first consider the mobility of the entire dissolved molecule, such as ionic mobility in polar liquids. When the relaxation time of the medium is sufficiently fast, the entire medium deformation follows the ion. However, as the ion's diffusion coefficient is increased, part of the deformation shell starts to lag behind, producing dielectric friction.[5,6] This lag concerns only collective polarization of the permanent dipoles, while induced dipoles still follow ion's diffusion adiabatically.

One can extend this argument a bit further by allowing the charge to tunnel quantum mechanically, as it happens in proton and electron transfer. For this very short time of the charge motion, the entire nuclear bath is dynamically frozen (Franck-Condon principle) and only the electronic subsystem adiabatically follows each tunneling event.

The Franck-Condon picture requires a separation of time scales. The first time is the period of electron oscillations between the donor and acceptor states: $\tau_{DA} \simeq \omega_{DA}^{-1}$, where $\omega_{DA} = \langle \Delta E \rangle / \hbar$ and $\langle \Delta E \rangle$ is the average energy gap between the acceptor and donor electronic states. It can be associated with the maximum of the charge-transfer absorption band in a spectroscopic experiment. If the electrons of the medium are characterized by the time-scale $\tau_f \simeq \omega_f^{-1}$ short compared to τ_{DA}, they will follow the electron adiabatically. The donor-acceptor energy gap thus needs to fall in the optical transparency window of the solvent, and ω_f refers to the optical absorption band of the solvent. The nuclear degrees of freedom are much slower than the electron and are dynamically frozen on the time-scale of electron's motion. The required separation of time scales is as follows: $\tau_n \gg \tau_{DA} \gg \tau_f$, where τ_n is the relaxation time of the nuclear modes responsible for the medium polarization.

It was Pekar,[3] who first proposed that the medium deformation stabilizing the charge must be associated with the electrostatic multipolar polarization caused by the Coulomb field of the electron. One can apply different levels of theory to capture this state of enhanced polarization relative to the nonpolarized medium. The simplest approach is to assume that the medium polarization is spread as a continuous field characterized by a

[a)] Electronic mail: dmitrym@asu.edu

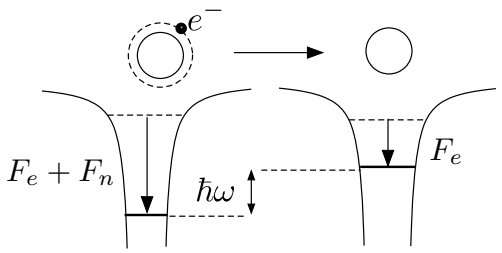

FIG. 1. Illustration of the different nature of the electronic, F_e, and nuclear, F_n, solvation free energies entering the problem of electronic transitions in condensed media. The initial equilibrium state at the donor (left) is stabilized by the entire equilibrium free energy $F_n + F_e$. When the energy $\hbar\omega$ is supplied, the electron moves to the acceptor energy level (right) shifted down by the electronic free energy F_e compared to the gas-phase energy level shown by the broken line (we do not label separately the initial and final solvation energies for simplicity). Nuclear relaxation follows the electron transfer event, sinking the acceptor level further down to the total free energy of solvation $F_n + F_e$.

dielectric susceptibility. To separate the nuclear polarization from the electronic polarization, one can introduce a separate continuous field of induced dipoles, as first done by Fröhlich.[7] It is characterized by the high-frequency dielectric constant ϵ_∞ measured by dielectric spectroscopy[8,9] at the frequency $\omega = \omega_f$, $\epsilon_\infty = \epsilon(\omega_f)$. The response of this electronic polarization to the electron's electric field is specified by the longitudinal susceptibility (superscript "L")

$$\chi_e^L = (4\pi)^{-1}(1 - \epsilon_\infty^{-1}). \tag{1}$$

The corresponding free energy of electronic polarization scales with this susceptibility as $-F_e \propto \chi_e^L$ (Fig. 1).

The initial state of the electron, if maintained sufficiently long, will polarize both the electronic and nuclear degrees of freedom. If the waiting, or preparation, time of this state is significantly longer than τ_n, the total dielectric polarization will scale with the zero-frequency susceptibility $\chi^L = (4\pi)^{-1}(1 - \epsilon_s^{-1})$ associated with the static dielectric constant $\epsilon_s = \epsilon(0)$. In the Pekar prescription,[3] the nuclear free energy of solvation $-F_n$, associated with relaxing the nuclear configuration of the solvent, scales with the difference of χ^L and χ_e^L,

$$\chi_P^L = (4\pi)^{-1} c_0. \tag{2}$$

Here, $c_0 = \epsilon_\infty^{-1} - \epsilon_s^{-1}$ is the Pekar factor.[3,10] In similar terms, dielectric friction to the diffusional motion of a solvated ion is caused by polarization waves dissipated to the nuclear degrees of freedom. The dielectric friction force,[5] $\propto c_0 \tau_L a^{-3}$, is proportional to c_0 and the longitudinal relaxation time τ_L and is inversely proportional to the cube of the ion radius a.

In theories of electron transfer, the nuclear polarization, which is dynamically uncoupled from the fast electron motions, produces fluctuations of the electrostatic potential that bring the donor-acceptor energy gap $X = \Delta E$ to zero. This is the condition for electron tunneling at the top of the activation barrier for an electron transfer reaction.[11–13] The probability of reaching this configuration is a Gaussian function with the average energy gap $\langle \Delta E \rangle$ and the energy gap variance $\sigma_X^2 = 2k_\mathrm{B}T\lambda$ characterized by the reorganization energy λ. Within the linear response approximation, λ needs to be associated with a free energy of solvation and the term "reorganization energy" is understood here in this sense. It can be calculated as the negative of the free energy of nuclear solvation of the "electron-transfer dipole", which is a fictitious solute with the repulsive core of the donor-acceptor complex producing the electric field in the environment equal to $\Delta\mathbf{E}_0 = \mathbf{E}_{02} - \mathbf{E}_{01}$. Here, $\mathbf{E}_{0i}$, $i = 1, 2$ is the electric field of the electron localized at either the donor ($i = 1$) or acceptor ($i = 2$). It is given in terms of the electronic wave function ψ_{0i} as

$$\mathbf{E}_{0i} = -\nabla \int \frac{|\psi_{0i}(\mathbf{r}')|^2}{|\mathbf{r} - \mathbf{r}'|} d\mathbf{r}'. \tag{3}$$

The standard choice of the states ψ_{0i} is from diabatic vacuum states. Loosely stated, diabatic states provide maximum localization of the electron on the donor and acceptor. A number of calculation algorithms have been proposed to define these states.[14] Suffice it to say here that the use of vacuum wave functions is justified for strongly bound molecular electronic states characterized by high ionization potentials. For polaron states,[3,4] the wave functions of the electrons in the polarized medium $\psi_i[\mathbf{P}]$ need to enter the electric field. The electron energy then becomes a nonlinear functional of the medium polarization solved by applying the variational principle.[3,4] The use of the vacuum basis set, as is typically employed in electron transfer theories, keeps the problem in the domain of linear models, which are quadratic functionals of the medium polarization and are characterized by the Gaussian distribution of the energy gap ΔE. The rest of this paper is focused on defining such quadratic functionals in the framework of either continuum or molecular discrete (microscopic) models of the solvent.

The reorganization energy λ, characterizing the breadth of fluctuations of the donor and acceptor energy levels, is a central parameter of electron-transfer theories. It is accessible from spectroscopy as half of the Stokes shift for the charge-transfer optical bands.[15,16] When the continuum model of the solvent polarization is adopted, λ scales linearly with the Pekar factor[11]

$$\lambda = c_0 g. \tag{4}$$

Here, g denotes the free energy of the vacuum electric field $\Delta\mathbf{E}_0$ in the volume Ω occupied by the polarized medium

$$g = (8\pi)^{-1} \int_\Omega \Delta\mathbf{E}_0^2 d\mathbf{r}. \tag{5}$$

For the simplified geometry of equal-size donor and acceptor particles with the radii R_d separated by the dis-

tance R one has from the above equations[11]

$$\lambda = e^2 c_0 \left[R_d^{-1} - R^{-1} \right]. \tag{6}$$

The Pekar factor in Eq. (4) plays the role of the solvation susceptibility $\chi_a^{\rm solv}$ (in contrast to the dielectric susceptibility). It connects, in the continuum limit, the free energy of solvation to the free energy of the solute vacuum field

$$F_a = -\tfrac{1}{2}\chi_a^{\rm solv} \int_\Omega \mathbf{E}_0 \cdot \mathbf{E}_0 d\mathbf{r}. \tag{7}$$

Here $a = e, n$ denotes either electronic ($a = e$) or nuclear ($a = n$) free energies. For the continuum reorganization energy, one has $\lambda = -F_n$, $\chi_n^{\rm solv} = \chi_P^L$, and $\mathbf{E}_0 = \Delta\mathbf{E}_0$.

As is seen from Eqs. (1) and (2), the Pekar prescription provides a simple link between the solvation susceptibility and dielectric susceptibilities of the polar liquid provided by dielectric spectroscopy. This link is established on the basis of quadratic polarization functionals describing Gaussian fluctuations of the liquid polarization near the equilibrium. The main focus of this work is on developing a consistent approach to define such functionals, and on the corresponding bulk susceptibilities of the homogeneous solvent. We additionally derive a connection between these bulk susceptibilities and the longitudinal solvation susceptibility entering the equation for the reorganization energy. The continuum limit for the microscopic solvation susceptibility is obtained from simulations and compared to χ_P^L in Eq. (2). This connection allows us to critically test the accuracy of $\lambda \propto c_0$ in Eq. (4).

There is a significant distinction of our approach from previous studies of solvation and electron transfer in polar solvents. It is often taken for granted that the result given by Eq. (4) is the only possible outcome of the continuum model of dielectrics, which all microscopic solutions are expected to approach when the continuum limit is taken. An early warning that this might be not true came from Brady and Carr,[17] who used a partitioning alternative to Pekar's. They showed that the nuclear solvation energy is sensitive to that choice,[18] but failed to recognize the important distinction between the longitudinal and transverse dielectric response.[19,20] We make here the next step forward and suggest, following an early proposal by Høye and Stell,[21] that a whole family of mean-field continuum results can be produced from the same microscopic Hamiltonian of the polar liquid. These different continua are achieved by taking $k = 0$ limit in microscopic nonlocal susceptibilities defined in the reciprocal space, which are connected by the fluctuation-dissipation theorem to fluctuations of the corresponding polarization fields.[22] These continuum susceptibilities enter, in turn, the macroscopic functionals specifying the reversible work (free energy) required to produce a nonequilibrium nuclear polarization of the medium in the presence of the solute.[23–25] The application of these functionals is two-fold. They can either be used to calculate the probability of a fluctuation out of equilibrium, bringing the system to the top of the activation barrier (electron transfer), or to find the free energy released by relaxing the system in response to the perturbation introduced by the solute (solvation).

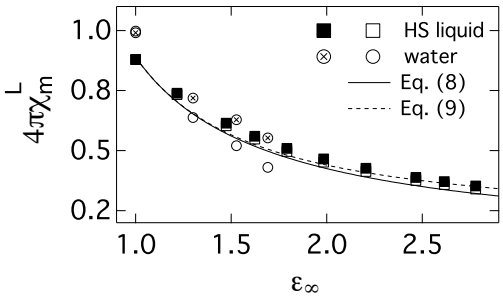

FIG. 2. Continuum longitudinal susceptibility $4\pi\chi_m^L$, entering the continuum reorganization energy, vs the high-frequency dielectric constant ϵ_∞. The standard Pekar formulation assumes $4\pi\chi_m^L = 4\pi\chi_P^L = c_0$ (Eq. (2), filled points). The continuum limit $4\pi\chi_m^L$ from numerical simulations is shown by the open points (open squares nearly coincide with the filled squares). Results for two types of polarizable fluids are shown: $N = 1000$ SWM4-DP water molecules (circles) and $N = 864$ dipolar polarizable hard spheres (HS) (squares). The reduced polarizability $\alpha^* = \alpha/\sigma^3$ (σ is the molecular diameter) was varied between 0.0 and 0.054 for SWM4-DP water ($\epsilon_s = 81$ at $\alpha^* = 0.044$) and between 0.0 and 0.1 for dipolar hard spheres ($\epsilon_s = 14$ at $\alpha^* = 0.04$). The dielectric constant was calculated from the Clausius-Mossotti equation [Eq. (43)] and the parameter y_e' [Eq. (73)], which is the condensed-phase analog of y_e in Eq. (10). The solid and dashed lines refer to Eqs. (8) and (9), respectively. The statistical errors of the simulations are smaller than the size of the points in the plot. The open and closed points overlap at $\epsilon_\infty = 1$.

Particularly important for the final result is the susceptibility related to cross correlations between the electronic and nuclear polarization of the liquid. The standard approach adopted in macroscopic polarization functionals is to assume that such cross correlations are limited to the Coulomb interaction between the electronic and nuclear polarization fields.[25] While this is obviously correct when applied to molecular permanent and induced dipoles, coarse graining of the molecular dipoles into continuous fields "dresses" the basic Coulomb interactions with the short-range correlations in the liquid. Felderhof showed[26] that a general fluctuation functional can be set up, with some generic forms for the self and cross susceptibilities between the electronic and nuclear polarization fields. However, one needs microscopic simulations or liquid-state theories to establish these susceptibilities. We use here the former approach to find susceptibilities consistent with the statistics of polar-polarizable fluids from atomistic simulations. Specifically, nonlocal susceptibilities from finite-size simulations of bulk polar-polarizable fluids are extrapolated to $k = 0$ to find their continuum values. This procedure is repeated for a set of

fluids with varying molecular polarizability α to obtain the dependence of extrapolated continuum susceptibilities on ϵ_∞. These results provide us with a critical test of Eq. (4).

The main result of our numerical simulations is shown in Fig. 2. It shows the continuum, $k \to 0$, limit χ_m^L of the microscopic (subscript "m") nuclear susceptibility calculated from numerical simulations. In the Pekar description one expects $\chi_m^L = \chi_P^L$, where χ_P^L is given by Eq. (2). $\chi_m^L(\epsilon_\infty)$ is calculated from simulations of two types of polarizable fluids: polarizable hard spheres carrying point permanent and induced dipoles ($\epsilon_s = 14$ at $\alpha^* = \alpha/\sigma^3 = 0.04$, σ is the molecular diameter) and polarizable water models carrying atomic partial charges and induced point dipoles ($\epsilon_s = 81$ at $\alpha^* = 0.044$). There is good numerical agreement between the Pekar susceptibility χ_P^L (filled points) and χ_m^L (open points). However, the derivation of χ_m^L from these nonlocal susceptibilities results in a quite distinct functional form

$$\chi_m^L = \frac{\epsilon_s - 1}{4\pi\epsilon_s}\left(\frac{\epsilon_\infty + 2}{3\epsilon_\infty}\right)^2. \tag{8}$$

This equation is shown by the solid line in Fig. 2. Despite a clearly different functionality, which now involves the product of functions of ϵ_∞ and ϵ_s instead of the difference of such functions in the Pekar factor, the two forms produce very close numerical values (solid line vs filled points). The structure of this equation will be discussed in more detail below. Briefly, it absorbs into itself the product of the longitudinal susceptibility of the polar liquid χ^L with the squared Lorentz screening[9] of the vacuum field by the induced dipoles. Since the reorganization energy depends quadratically on the solute field [Eq. (5)], the screening factor is squared in χ_m^L.

Deriving Eq. (8) involves some approximations discussed below. A slightly better account of the simulation data is provided by an alternative formula

$$\chi_m^L = \frac{\epsilon_s - 1}{4\pi\epsilon_s}\frac{1}{(1 + 2y_e)^2}, \tag{9}$$

where

$$y_e = (4\pi/3)\rho\alpha, \tag{10}$$

ρ is the number density and α is the gas-phase molecular polarizability. This second relation is shown by the dashed line in Fig. 2.

Equations (8) and (9) produce comparable results in the range of ϵ_∞ typical for molecular liquids. One can arrive at Eq. (8) from Eq. (9) by using one of the forms of the Clausius-Mossotti equation adopted in the literature: $(\epsilon_\infty - 1)/(\epsilon_\infty + 2) = y_e$. We, however, will replace y_e in the latter equation with the condensed-phase parameter y_e'. It is based on the condensed-phase polarizability α',[27–29] instead of the gas-phase polarizability α in Eq. (10). This distinction is the cause of a slight numerical difference between Eqs. (8) and (9).

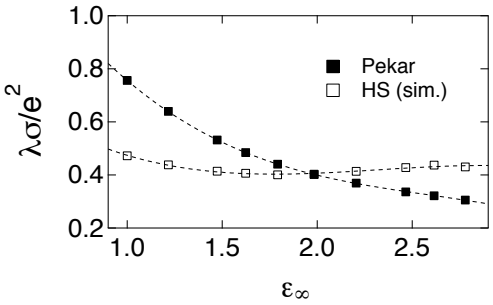

FIG. 3. The reorganization energy (normalized with e^2/σ) obtained from the Marcus formula [Eq. (6)] ($R_d/\sigma = 0.8$, $R = 2R_d$, filled squares) and from k-integration (Eq. (84), $R_1/\sigma = R_d/\sigma + 0.5 = 1.3$, $R = 2R_1$, open squares) with nonlocal susceptibilities obtained from simulations (sim.) of hard-sphere (HS) fluids with increasing polarizability α and a constant permanent dipole moment m (σ is the HS diameter). The results of calculations are plotted against ϵ_∞ calculated from simulations. The dashed lines are regressions drawn through simulation points to guide the eye.

The nonlocal, reciprocal-space susceptibilities obtained from simulations are used to calculate the reorganization energy of electron transfer by integrating them with the reciprocal-space electric field of the electron-transfer dipole. The main result of these calculations is that the dependence of λ on ϵ_∞ suggested by Eq. (4) is not supported (see discussion below in connection to Eq. (84)). If one takes a strongly polar solvent with $\epsilon_s \gg 1$, one can neglect ϵ_s in the Pekar factor with the result $\lambda \simeq \epsilon_\infty^{-1} g$. This simple prediction implies that the reorganization energy should decrease by a factor of about two in going from a non-polarizable liquid with $\epsilon_\infty = 1$ to a polarizable liquid with the typical value $\epsilon_\infty \simeq n^2 \simeq 2$ (Figs. 2 and 3), where n is the refractive index (ϵ_∞ might deviate from n^2, water is a notable example[30]).

We find that λ is nearly constant with increasing ϵ_∞, instead of the predicted decrease, for polarizable dipolar fluids (open vs filled squares in Fig. 3). This result is qualitatively consistent with previous simulations of similar fluids solvating a spherical dipole[31] and calculations done on more complex solutes.[32] In the case of polarizable water, the reorganization energy noticeably increases in simulations, in contrast to the decrease predicted by the Pekar susceptibility (open vs filled circles in Fig. 4). The deviation between microscopic and continuum results is controlled by the solute size R_d relative to the solvent diameter σ. The two sets of calculations converge in the limit $R_d/\sigma \gg 1$.

II. Continuum polarization functionals

We start by introducing notations used throughout the paper. A number of vector (tensor) and scalar fields enter integrals over the space occupied by the polarized liquid. In order to avoid multiple use of integrals and tensor contractions, we use asterisks between tensorial fields to denote both the truncation over common indexes and

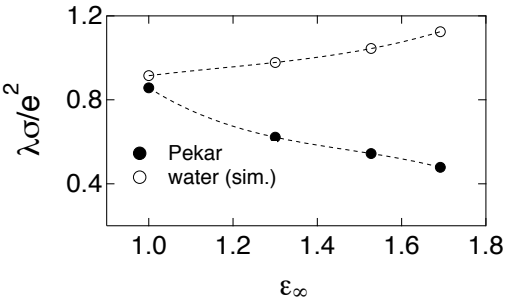

FIG. 4. The reorganization energy obtained from the Marcus formula [Eq. (6)] ($R_d/\sigma = 0.8$, $R = 2R_d$, filled points) and from k-integration (Eq. (84), $R_1/\sigma = R_d/\sigma + 0.5 = 1.3$, $R = 2R_1$, open squares) with nonlocal susceptibilities obtained from simulations (sim.) of SWM4-DP water with varying dipolar polarizability (the HS diameter is $\sigma = 2.87$ Å). The dashed lines are regressions drawn through simulation points to guide the eye.

integration over the space occupied by the liquid. In this notation, the integral between the rank two tensor $\mathbf{T}(\mathbf{r}-\mathbf{r}')$ and the rank one tensor $\mathbf{P}(\mathbf{r}')$ will produce a vector field $\mathbf{E}(\mathbf{r})$ with the notation

$$\mathbf{E} = \mathbf{T} * \mathbf{P}'. \tag{11}$$

This shorthand form implies in the standard integral notation

$$E_\alpha(\mathbf{r}) = \int_\Omega T_{\alpha\beta}(\mathbf{r}-\mathbf{r}')P_\beta(\mathbf{r}')d\mathbf{r}', \tag{12}$$

where α, β denote the Cartesian components and summation over the common indexes is assumed; Ω is the volume occupied by the polar liquid (solvent). Likewise, when prime is not involved in the contraction, it implies that the result is a scalar quantity, such that

$$\mathbf{P} * \mathbf{P} = \int_\Omega \mathbf{P}(\mathbf{r}) \cdot \mathbf{P}(\mathbf{r}) d\mathbf{r}. \tag{13}$$

We will mostly follow the shorthand notation outlined in Eqs. (11) and (13), but occasionally use the standard integral representation in cases when the short form can potentially create confusion. In those cases, the dot product, such as $\mathbf{P} \cdot \mathbf{P}$, is the standard notation for contraction, $P_\alpha P_\alpha$, producing a scalar field.

We will also use below reciprocal-space fields obtained by the Fourier transform of the direct-space fields. Those are denoted with tilde, such as $\tilde{\mathbf{P}}$. Correspondingly, the contraction of reciprocal-space fields corresponds to the following integral

$$\tilde{\mathbf{P}} * \tilde{\mathbf{P}} = \int \frac{d\mathbf{k}}{(2\pi)^3} \tilde{\mathbf{P}}(\mathbf{k}) \cdot \tilde{\mathbf{P}}(\mathbf{k}). \tag{14}$$

In this notation scheme, the free energy of electronic ($a = e$) or nuclear ($a = n$) solvation of a generic solute placed in a polar solvent schematically shown in Fig. 1 is given by the relation

$$F_a = -\tfrac{1}{2}\chi_a^{\mathrm{solv}}(k) * |\tilde{\mathbf{E}}_0|^2, \tag{15}$$

where $\mathbf{E}_0$ specifies the (vacuum) electric field of external charges, which are typically atomic (partial) charges located inside the solute. The solvation susceptibility function $\chi_a^{\mathrm{solv}}(k)$ here is nonlocal and depends on the wavevector k. Taking the $k \to 0$ limit in this function produces the continuum solvation susceptibility $\chi_a^{\mathrm{solv}} = \chi_a^{\mathrm{solv}}(0)$ and the continuum free energies in Eq. (7). Our main focus below is on the longitudinal microscopic susceptibility $\chi_m^L(k)$. We start with defining free energy functionals of the polarization fields and the corresponding bulk susceptibilities, eventually leading to the solvation free energies.

A. Total polarization density

The first non-equilibrium functional broadly used in the literature devoted to solvation, spectroscopy, and electron transfer was due to Marcus.[23,33] The actual derivation by Marcus distinguishes between the fast and slow components of the polarization density field $\mathbf{P}$,[23] as we discuss below, but if this distinction is not made explicit at first, the Marcus functional can be written as

$$F[\mathbf{P}] = \frac{1}{2\chi^L}\mathbf{P} * \mathbf{P} - \mathbf{E}_0 * \mathbf{P}. \tag{16}$$

The need to distinguish between the longitudinal (L) and transverse (T) susceptibilities of the bulk solvent[29,34–37] is explained below when the proper $k \to 0$ limit is introduced in the reciprocal-space nonlocal susceptibilities.

The free energy $F[\mathbf{P}]$ specifies the reversible constant-volume work required to create in the system composed of the solute and solvent a non-equilibrium polarization $\mathbf{P}$. The equilibrium polarization $\mathbf{P}_{\mathrm{eq}}^L = \chi^L \mathbf{E}_0$ follows from minimizing the functional. The consistency with this expected limit and the harmonic form, consistent with the Gaussian distribution of the fluctuating macroscopic variable $\mathbf{P}$, are incorporated in the Marcus functional. This functional, and other constructs pursuing similar goals, can be viewed as different approximations for the exact definition, which can be set up in terms of the collective coordinate of the total microscopic polarization density of the liquid $\mathbf{P}(\mathbf{r}) = \sum_j (\mathbf{m}_j + \mathbf{p}_j)\delta(\mathbf{r} - \mathbf{r}_j)$, $\mathbf{m}_j$ and $\mathbf{p}_j$ are, correspondingly, the permanent and induced molecular dipoles of the liquid. This collective coordinate is projected from the entire phase space of the system Γ by weighting the δ-function with the Boltzmann factor given in terms of the system Hamiltonian H

$$e^{-\beta F[\mathbf{P}]} = \int \delta\left(\mathbf{P} - \sum_j (\mathbf{m}_j + \mathbf{p}_j)\delta(\mathbf{r} - \mathbf{r}_j)\right) e^{-\beta H} d\Gamma, \tag{17}$$

where $\beta = 1/(k_{\mathrm{B}}T)$ is the inverse temperature.

An alternative expression was proposed by Felderhof[24] based on the requirement that minimizing the functional

should produce the Maxwell equation

$$F[\mathbf{P}] = \frac{1}{2\chi^T}\mathbf{P}*\mathbf{P} + \tfrac{1}{2}\nabla'\cdot\mathbf{P}' * \frac{1}{|\mathbf{r}'-\mathbf{r}''|} * \nabla''\cdot\mathbf{P}'' - \mathbf{E}_0 * \mathbf{P}, \tag{18}$$

where the transverse susceptibility of the bulk polar liquid $\chi^T = (\epsilon_s - 1)/(4\pi)$ now appears in the harmonic polarization term, in contrast to χ^L in the Marcus functional. Indeed, minimizing this functional results in the Maxwell constitutive relation $\mathbf{P}_{\rm eq} = \chi^T\mathbf{E}$, where the Maxwell field $\mathbf{E}$ combines $\mathbf{E}_0$ and the field of the bound charges at the liquid molecules

$$\mathbf{E} = \mathbf{E}_0 - \nabla\int\frac{\rho'_b}{|\mathbf{r}-\mathbf{r}'|}d\mathbf{r}', \quad \rho'_b = -\nabla'\cdot\mathbf{P}'. \tag{19}$$

An alternative form of the Felderhof functional in terms of fields $\mathbf{P}$ and the dielectric displacement $\mathbf{D} = \mathbf{E} + 4\pi\mathbf{P}$ was suggested by Maggs and Everaers[38]

$$F[\mathbf{P}] = \frac{1}{2\chi^T}\mathbf{P}*\mathbf{P} + \frac{1}{8\pi}(\mathbf{D}-4\pi\mathbf{P})*(\mathbf{D}-4\pi\mathbf{P}). \tag{20}$$

It has been noted in the past[25,39–41] that the Marcus and Felderhof expressions can be partially reconciled by the use of the Helmholtz theorem representing a general vector field as the sum of the longitudinal (irrotational, L) and transverse (solenoidal, T) projections,[42] $\mathbf{P} = \mathbf{P}^L + \mathbf{P}^T$, such that $\mathbf{P}^L * \mathbf{P}^T = 0$. The transformation is based on the identity replacing the Coulomb interaction of the molecular bound charges with the integral over the longitudinal projection of the polarization field

$$\nabla'\cdot\mathbf{P}' * \frac{1}{|\mathbf{r}'-\mathbf{r}''|} * \nabla''\cdot\mathbf{P}'' = 4\pi\mathbf{P}^L * \mathbf{P}^L. \tag{21}$$

Applying this identity to the Felderhof functional in Eq. (18) transforms it into

$$F[\mathbf{P}] = \frac{1}{2\chi^T}\mathbf{P}^T*\mathbf{P}^T + \frac{1}{2\chi^L}\mathbf{P}^L*\mathbf{P}^L - \mathbf{E}_0*\mathbf{P}. \tag{22}$$

The Marcus functional in Eq. (16), therefore, does not recognize the distinction between the longitudinal and transverse projections of the fields involved.[39] This problem does not show up in applications assuming the longitudinal character of the external field, $\mathbf{E}_0 = \mathbf{E}_0^L$.

According to the Helmholtz theorem, the longitudinal projection of any vector field $\mathbf{A}$ is given as[42]

$$4\pi\mathbf{A}^L = -\nabla\int\frac{\nabla'\cdot\mathbf{A}'}{|\mathbf{r}-\mathbf{r}'|}d\mathbf{r}'. \tag{23}$$

From this equation, the Maxwell field becomes[41,43,44]

$$\mathbf{E} = \mathbf{E}_0 - 4\pi\mathbf{P}^L. \tag{24}$$

This relation can be used in Eq. (21) to rewrite Felderhof's functional in an alternative form

$$F[\mathbf{P}] = \frac{1}{2\chi^T}\mathbf{P}*\mathbf{P} - \tfrac{1}{2}(\mathbf{E}_0+\mathbf{E})*\mathbf{P}^L - \mathbf{E}_0*\mathbf{P}^T. \tag{25}$$

If one assumes that the external field is longitudinal, $\mathbf{E}_0 = \mathbf{E}_0^L$, the last term in the above equation vanishes by symmetry (Helmholtz theorem) and one arrives at the Marcus functional as given in Refs. 23 and 40. This functional is defined in terms of three fields, $\mathbf{P}$, $\mathbf{E}$ and $\mathbf{E}_0$, while only two are in fact required, as in Eqs. (20) and (22).

The manipulations shown here indicate that different functionals developed over the years can be transformed into each other when one assumes that the field of the external charges is longitudinal. While the bare Coulomb field of charges external to the dielectric is always longitudinal, this assumption is not justified for many cases when the charges are placed inside a cavity carved from the dielectric. As a matter of fact, the assumption of the longitudinal external field is never justified when electron is transferred between the donor and acceptor.

The imposition of the repulsive core of the solute or, in other words, the restriction imposed on the volume over which the field is integrated creates a transversal component of the field and a corresponding transverse polar response. This component is non-zero any time the symmetry of the cavity does not coincide with the symmetry of the field,[45] or, in the dielectric boundary value problem, when the cavity surface does not coincide with the equipotential surface.[46] A direct consequence of this situation is that the vacuum field $\mathbf{E}_0$ does not coincide with $\mathbf{D}$.[47,48] Note that, per Eq. (24), the longitudinal projections of the two fields always coincide, $\mathbf{D}^L = \mathbf{E}_0^L$. This relation can be used to demonstrate the equivalence of the Felderhof and Maggs-Everaers functionals.

The transverse component is absent for an ion at the center of a spherical cavity or for the polarization of an infinite dielectric slab by a uniform external field. In both cases, the dielectric dividing surface coincides with the equipotential surface. There is a very limited number of configurations where this condition can be satisfied. For any configuration involving transferring a charge, the equipotential surface of the "charge-transfer dipole", i.e., of the difference field $\Delta\mathbf{E}_0$ between the final and initial states, never coincides with the cavity surface. Transverse component of the response is required for any such problem and the restriction of using longitudinal fields is always an approximation.

A simple example that amply demonstrates these difficulties is solvation of the dipole m_0 placed at the center of a spherical cavity. The famous Onsager (continuum) result for the solvation free energy[27] requires both longitudinal and transverse susceptibilities of bulk solvent to enter the overall solvation free energy[45]

$$\Delta F_s = -\frac{4\pi m_0^2}{a^3}\frac{\chi^T\chi^L}{\chi^L + 2\chi^T}, \tag{26}$$

where a is the cavity radius. The solvation susceptibility in this expression becomes a complex and nonlinear function of the longitudinal and transverse dielectric susceptibilities. The expression in the denominator of this formula is the trace of the susceptibility, $\chi = \chi^L + 2\chi^T$. It is

connected to the variance of the macroscopic dipole moment of the liquid $\mathbf{M}$ by the Kirkwood-Onsager equation[7] (see Eq. (4.58a) in Ref. 28)

$$\chi = \frac{(\epsilon_s - 1)(2\epsilon_s + 1)}{4\pi\epsilon_s} = \frac{\beta}{\Omega}\langle(\delta\mathbf{M})^2\rangle, \qquad (27)$$

where $\delta\mathbf{M} = \mathbf{M} - \langle\mathbf{M}\rangle$. The dipole moment $\mathbf{M} = \sum_j(\mathbf{m}_j + \mathbf{p}_j)$ here is the sum of all permanent and induced dipoles in the liquid.[28] The variance of the dipole moment is calculated over the configurations of bulk liquid in the absence of any external fields.

As mentioned above, the description of quantum transitions requires separation of the liquid polarization into a fast electronic and slow nuclear components.[23,49,50] The slow component can fluctuate out of equilibrium with the electronic charge distribution producing inhomogeneous broadening of the spectral lines. Before we proceed to explicit separation schemes, it is useful to point out the difficulties of all such separation schemes, which originate from the quadratic form of the polarization functional.

Minimizing the Felderhof functional in Eq. (25) produces the equilibrium free energy

$$F_{\rm eq} = -\mathbf{E_0}^L * \mathbf{P}^L_{\rm eq} + \frac{1}{2\chi^L}\mathbf{P}^L_{\rm eq} * \mathbf{P}^L_{\rm eq}. \qquad (28)$$

The first term in this equation, $\langle E\rangle = -\mathbf{E}^L_0 * \mathbf{P}^L_{\rm eq}$ is the equilibrium energy of the solute-solvent interaction (not equal to the solvation energy[51]). It is obvious that this energy does not depend on how $\mathbf{P}^L_{\rm eq}$ is separated into components and is therefore invariant to different separation schemes.[18] The second term, the polarization of the medium, is quadratic in the polarization field and is affected by the cross term between the polarization components. When the susceptibility in the components space is given by a matrix, including the self (diagonal) and cross (off-diagonal) matrix elements, the free energy becomes non-additive in terms of the polarization components, in contrast to the average solute-solvent energy. For the purpose of characterizing one component of the free energy, which is the nuclear free energy of slow polarization in our case, the separation scheme affects the outcome.

B. Electronic and nuclear components

The overall vector field $\mathbf{P}$ is now separated into the electronic, $\mathbf{P}_e$, and nuclear, $\mathbf{P}_n$, components: $\mathbf{P} = \mathbf{P}_e + \mathbf{P}_n$. While the separation of these components in the free energy functional was discussed by Pekar[3,10] and Marcus[33] a clear exposure to the problem was presented by Lee and Hynes,[25] which we follow here. The Lee-Hynes functional is a direct extension of the Felderhof functional in Eq. (22) to a two-component polarization field (Eq. (A3) in Ref. 25)

$$F[\mathbf{P}_e, \mathbf{P}_n] = \sum_{a=e,n}\frac{1}{2\chi^T_a}\mathbf{P}_a{*}\mathbf{P}_a + 2\pi\mathbf{P}^L{*}\mathbf{P}^L - \mathbf{E}_0{*}\mathbf{P}, \quad (29)$$

where we do not require the longitudinal character of the external vacuum field $\mathbf{E}_0$. The separate electronic and nuclear susceptibilities are given as $\chi^T_e = (\epsilon_\infty - 1)/(4\pi)$ and $\chi^T_n = (\epsilon_s - \epsilon_\infty)/(4\pi)$. We note in passing that exactly the same equation follows from the Marcus functional involving two separate polarization components when Eq. (24) is applied to it (see, e.g., Eq. (80) in Ref. 23). The corresponding functional in the Pekar formulation[10] avoids the coupling between the electronic and nuclear polarization fields and has the following form

$$F_P[\mathbf{P}_e, \mathbf{P}_n] = \frac{1}{2\chi^L_P}\mathbf{P}^L_n{*}\mathbf{P}^L_n + \frac{1}{2\chi^L_e}\mathbf{P}^L_e{*}\mathbf{P}^L_e - \mathbf{E}_0{*}\mathbf{P}^L. \quad (30)$$

The neglect of the cross term in the Pekar functional, while not physically justified, can be vindicated on the mathematical grounds since a quadratic functional can be diagonalized by a unitary transformation as long as the final observable properties are not affected. We show below that indeed the Pekar and Lee-Hynes functionals produce the same expression for the solvent reorganization energy of electron transfer.

Although different quadratic functionals can often be transformed into each other, they are not always consistent in their surface terms. Correct expression is obtained from the functionals given by Kim and Hynes (Eq. (2.1) in Ref. 52) and by Aguilar *et al* (Eq. (28) in Ref. 49). The surface term

$$F_S[\mathbf{P}_e, \mathbf{P}_n] = -\tfrac{1}{2}\mathbf{P} * \mathbf{E}_\sigma \qquad (31)$$

needs to be added to the volume functional in Eq. (29), where $\mathbf{E}_\sigma$ is the field of the surface charge density $\sigma(\mathbf{r}_S) = \hat{\mathbf{n}}_S \cdot \mathbf{P}(\mathbf{r}_S)$ created at the surface S of the solute by the discontinuous polarization density,[53] $\hat{\mathbf{n}}_S$ is the surface normal pointing outward from the dielectric.[54]

The surface term is required for the correct expression of the field inside the solute cavity. Minimizing $F[\mathbf{P}_e, \mathbf{P}_n] + F_S[\mathbf{P}_e, \mathbf{P}_n]$ in terms of $\mathbf{P}_e$ yields the equilibrium electronic polarization $\mathbf{P}^{\rm eq}_e$

$$\mathbf{P}^{\rm eq}_e = \chi^L_e\left[(\mathbf{E}_0 + \mathbf{E}_\sigma) - 4\pi\mathbf{P}_n\right]. \qquad (32)$$

It is in equilibrium with both the electric field and with the nuclear polarization, which is usually labeled as the Marcus partitioning.[18]

When the polarization density is projected on the solute-solvent dividing surface S, one obtains the surface charge density, $\sigma_e = \hat{\mathbf{n}}_S \cdot \mathbf{P}^{\rm eq}_e(\mathbf{r}_S) = \chi^L_e\left[E_{0n} + E_{\sigma n} - 4\pi\sigma_n\right]$, $\sigma_n = \hat{\mathbf{n}}_S \cdot \mathbf{P}_n(\mathbf{r}_S)$. Since the electric field of the bulk is zero inside the cavity, per Eq. (24), the field is the sum of the solute field $\mathbf{E}_0$ and the field of the surface charges $\mathbf{E}_\sigma$.[44] This is Eq. (17) from Ref. 49. It establishes the partitioning of the surface charge between electronic and nuclear polarization fields in polarized continuum models (PCM) of quantum mechanics. It is clear from this derivation, and from similar arguments presented in Ref. 49, that the formulation of the PCM adopted in the literature[55] is based on the Lee-Hynes polarization functional in Eq. (29) with the addition of the surface term in Eq. (31). If the polarization functional is modified, then the PCM formalism

requires modification as well. We show below that this is indeed the case and the Lee-Hynes functional in Eq. (29) is not consistent with microscopic simulations of polarizable fluids.

A particular problem area common to all currently used functionals is a somewhat simplistic account of the interaction between the electronic and nuclear polarization fields. Neglecting the surface terms, the cross induced-nuclear term in the Lee-Hynes functional in Eq. (29) is (see Eq. (21))

$$4\pi\mathbf{P}_e^L * \mathbf{P}_n^L = \nabla' \cdot \mathbf{P}'_e * \frac{1}{|\mathbf{r}' - \mathbf{r}''|} * \nabla'' \cdot \mathbf{P}''_n, \qquad (33)$$

which is the Coulomb interaction between the corresponding densities of the bound charge. As we have mentioned above and show more specifically below, coarse graining of the microscopic polarization into continuous fields "dresses" the direct Coulomb interactions with short-ranged correlations specific to the local liquid structure. The result is the appearance of cross susceptibilities that are distinct from the direct Coulomb interaction.

The non-equilibrium functional in Eq. (29) considers the fast electronic bath as projected on the classical vector field $\mathbf{P}_e$. The more precise approach is to define the instantaneous energy levels of the quantum subsystem by tracing out the fast electronic degrees of freedom in the density matrix defined through the system Hamiltonian H

$$e^{-\beta E[P_n]} = \mathrm{Tr_e}\left[e^{-\beta H}\right], \qquad (34)$$

where the trace, $\mathrm{Tr_e}$, is taken over the electronic quantum states of the bath. For the bath of harmonic oscillators (or polarizable Drude particles) the result of this procedure is equivalent to taking the functional integral over the polarization field[56] $\mathbf{P}_e$ and the corresponding canonically conjugate momentum $\mathbf{\Pi}_e$

$$e^{-\beta E[P_n]} \propto \int \mathcal{D}\mathbf{P}_e \mathcal{D}\mathbf{\Pi}_e e^{-\beta F[\mathbf{P}_e, \mathbf{P}_n]}. \qquad (35)$$

Taking the trace over the fast electronic degrees of freedom establishes the non-polar component of the free energy functional. When the classical trace is adopted in Eq. (35) by neglecting the integral over $\mathbf{\Pi}_e$, one obtains the free energy of induction solute-solvent interactions. When quantum induced dipoles are allowed (such as through the quantum Drude oscillators[57,58]), one obtains, in addition, dispersion (generally non-pairwise) solute-solvent interactions.[56] One can avoid calculating the integral over the classical polarization field by noting that for a harmonic functional $F[\mathbf{P}_e, \mathbf{P}_n]$ taking the functional integral in Eq. (35) is equivalent to minimizing $F[\mathbf{P}_e, \mathbf{P}_n]$ in respect to $\mathbf{P}_e$. Such minimization produces the instantaneous partial free energy of the electronic state $E[\mathbf{P}_n]$, depending on the non-equilibrium polarization $\mathbf{P}_n$ and the equilibrium electronic polarization of the thermal bath.

The minimization in respect to $\mathbf{P}_e$ can be done in the Lee-Hynes functional separately for the longitudinal and transverse projections. We will present the results for the longitudinal component only, as is commonly done in the literature.[25,40] The functionals discussed here in fact cannot be used in application to solvation by transverse polarization since they produce the "transverse catastrophe" of diverging solvation energy at $\epsilon_s \to \infty$. The transverse component of the susceptibility has to be renormalized by accounting for the repulsive core of the solute to avoid the divergence[45,59] (see below).

When only the longitudinal external field is considered, one gets the following expression for the non-equilibrium functional of the longitudinal nuclear polarization $\mathbf{P}_n^L$

$$F[\mathbf{P}_n^L] = F_e + \frac{1}{2\epsilon_\infty^2 \chi_P^L}\mathbf{P}_n^L * \mathbf{P}_n^L - \frac{1}{\epsilon_\infty}\mathbf{E}_0^L * \mathbf{P}_n^L, \qquad (36)$$

where $F_e = -(\chi_e^L/2)\mathbf{E}_0^L * \mathbf{E}_0^L$ is the equilibrium solvation free energy by the electronic polarization with the susceptibility given by Eq. (1).

One can use the non-equilibrium Lee-Hynes functional to specify the reorganization energy of electron transfer λ. One proceeds by replacing $\mathbf{E}_0^L$ by the difference of vacuum fields $\Delta\mathbf{E}_0^L$ in the two states to calculate the negative of the nuclear free energy of the solute charges screened by the fast electronic polarization

$$\lambda = \tfrac{1}{2}\epsilon_\infty^{-1}\Delta\mathbf{E}_0^L * \Delta\mathbf{P}_{n,\mathrm{eq}}^L. \qquad (37)$$

According to Eq. (36), the nuclear polarization $\Delta\mathbf{P}_{n,\mathrm{eq}}^L$ in equilibrium with $\epsilon_\infty^{-1}\Delta\mathbf{E}_0^L$ is $\Delta\mathbf{P}_{n,\mathrm{eq}}^L = (\epsilon_\infty c_0/4\pi)\Delta\mathbf{E}_0^L$ and one obtains Eq. (4).

Despite its insignificance for the final reorganization energy, the factor ϵ_∞^{-1} in front of the vacuum electric field in Eq. (36) carries an important physical meaning. It describes screening of the field of external charges by the electronic polarization of the medium continuously distributed throughout the solvent volume and characterized by the dielectric constant ϵ_∞.[52,60] As is usually true for dielectric models, dielectric screening depends on the specifics of the dielectric boundary value problem. This ambiguity creates some uncertainties in defining the screening function, as we discuss next. The full resolution of the problem requires truly microscopic calculations presented later in the text. However, it is useful to expose the difficulties encountered with adopting the model of continuously distributed electronic polarization (going back to Fröhlich[7]) by considering a hybrid model first, in which the permanent dipoles are treated at the molecular level, but the electronic polarization is continuous.[61]

C. Mean-field approximation

The hybrid model we want to briefly discuss here assumes permanent molecular dipoles of a liquid described at the microscopic level immersed in the continuum of high-frequency polarization $\mathbf{P}_e$. The corresponding free

energy functional becomes

$$F[\{\mathbf{m}\},\mathbf{P}_e] = F_e[\mathbf{P}_e] - \sum_j \mathbf{E}_{0j}\cdot\mathbf{m}_j - \tfrac{1}{2}\sum_{j\neq k}\mathbf{m}_j\cdot\mathbf{T}_{jk}\cdot\mathbf{m}_k, \tag{38}$$

where $\mathbf{E}_{0j} = \mathbf{E}_0[\mathbf{r}_j]$ and $\mathbf{T}_{jk}$ is the dipolar tensor[28] describing dipolar interactions between permanent dipoles $\mathbf{m}_j$. The free energy functional depending on the electronic polarization density $F_e[\mathbf{P}_e]$ is given by the relation

$$F_e[\mathbf{P}_e] = \frac{1}{2\chi_e^L}\mathbf{P}_e * \mathbf{P}_e - \mathbf{P}_e * \left[\mathbf{E}_0 + \sum_k \bar{\mathbf{T}}(\mathbf{r}-\mathbf{r}_k)\cdot\mathbf{m}_k\right]. \tag{39}$$

In this equation, the dipolar tensor $\bar{\mathbf{T}}$ connecting the continuously distributed electronic polarization with molecular permanent dipoles requires careful definition since it in fact involves boundary conditions for the electronic polarization in contact with the molecular dipole. The most elegant approach to deal with this problem was proposed by Høye and Stell[21] who noted that adding a constant parameter to the interaction potential inside the repulsive molecular core allows one to generate essentially all known mean-field theories of polar liquids, including the Onsager theory[27] and Wertheim's mean-spherical solution for dipolar hard spheres.[62] The definition of the dipolar tensor that allows one to achieve this goal is[21]

$$\bar{\mathbf{T}}(\mathbf{r}) = \mathbf{T}(\mathbf{r})\theta(r-\sigma) - (\Theta/\sigma^3)\theta(\sigma-r). \tag{40}$$

In this equation, $T_{\alpha\beta}(\mathbf{r}) = \nabla_\alpha\nabla_\beta(1/r)$ and $\theta(x)$ is the Heaviside function specifying the repulsive core of the molecule with the effective hard-sphere diameter[63] σ. The parameter Θ specifies a constant interaction potential inside the molecular core $r<\sigma$, which is arbitrarily added to the pairwise dipole-dipole interaction potential and does not affect any correlation functions in the liquid. However, this parameter affects the long-ranged, $k\to 0$, behavior of the liquid polarization, i.e., the mean-field limit of how the continuous electronic polarization responds to both permanent dipoles of the liquid and the external field of the solute.[21]

The free energy functional given by Eqs. (39) and (40) can now be used in Eq. (35) to integrate the electronic polarization field out. The result is the standard Hamiltonian of a fluid of permanent dipoles, with both dipole-dipole interactions and the interaction of the dipoles with the external field screened by the electronic polarization[61]

$$E[\{\mathbf{m}\}] = F_e - q\sum_j \mathbf{E}_{0j}\cdot\mathbf{m}_j - \tfrac{1}{2}p\sum_{j\neq k}\mathbf{m}_j\cdot\mathbf{T}_{jk}\cdot\mathbf{m}_k. \tag{41}$$

The screening functions q and p depend both on ϵ_∞ and the parameter Θ

$$\begin{aligned} q &= \frac{\epsilon_\infty(1-\Theta)+(2+\Theta)}{3\epsilon_\infty},\\ p &= \frac{2\epsilon_\infty(1-\Theta)+(1+2\Theta)}{3\epsilon_\infty}. \end{aligned} \tag{42}$$

The screening parameter of the Lee-Hynes functional, $q=\epsilon_\infty^{-1}$, is recovered at $\Theta=1$. This value of Θ is, however, unrealistic for dense polarizable materials. This is seen from the formula[21] connecting Θ to the dielectric constant ϵ_∞

$$\frac{\epsilon_\infty-1}{\epsilon_\infty+2} = \frac{y_e}{1+\Theta y_e}, \tag{43}$$

where y_e is given by Eq. (10). From Eq. (43), $\Theta=1$ corresponds to the dielectric constant of the polarizable ideal gas, $\epsilon_\infty = 1+3y_e$. On the contrary, $\Theta=0$ leads to the Clausius-Mossotti equation (Clausius-Mossotti continuum[21]), which describes well ϵ_∞ of dense polarizable liquids. Note that one gets the Lorentz screening factor[9] $q=(\epsilon_\infty+2)/(3\epsilon_\infty)$ at $\Theta=0$. The same screening parameter is obtained below when the continuum limit is taken in the microscopic screening function calculated from simulations. Our general result is that $\Theta=0$ is consistent with the simulations of polarizable fluids.

The calculations leading to Eq. (41) are useful in establishing the ingredients of the theory required to account for the electronic polarization in non-equilibrium polarization functionals. Such models are, however, not expected to be accurate in an attempt to answer the question of how the nuclear solvation free energy (such as λ) is varied with ϵ_∞. What Eq. (41) misses is that increasing the polarizability of the solvent also enhances the effective molecular dipole,[28] thus effectively counterbalancing the screening of electrostatic interactions.[31] Such effects cannot be consistently described by assuming one of the polarization fields (usually the electronic polarization[61]) to be continuous. A fully microscopic approach is required.

III. Microscopic functionals

Our point of departure in developing the microscopic formulation is the density functional discussed by Chandra and Bagchi.[39] It gives a formally exact expression for the functional of the microscopic density of the polar liquid $\rho(1)$ depending on the position $\mathbf{r}_1$ and orientation $\boldsymbol{\omega}_1$ of the molecule: $1=\{\mathbf{r}_1,\boldsymbol{\omega}_1\}$. The free energy invested to create the deviation $\delta\rho(1)=\rho(1)-\rho_{\rm eq}$ of the microscopic density from the equilibrium uniform density $\rho_{\rm eq}=\rho/(4\pi)$ is written as follows

$$\begin{aligned} \beta F[\delta\rho] = &\int d1\,(\rho(1)\ln(\rho(1)/\rho_{\rm eq}) - \delta\rho(1))\\ &- \tfrac{1}{2}\int \delta\rho(1)\delta\rho(2)c(12)d1d2 - \beta\mathbf{E}_0 * \mathbf{P}. \end{aligned} \tag{44}$$

Here, $d1 = d\mathbf{r}_1 d\boldsymbol{\omega}_1$ and the microscopic polarization density is defined as $\mathbf{P} = m\int \hat{\mathbf{e}}(1)\delta\rho(1)d\boldsymbol{\omega}_1$; $\hat{\mathbf{e}}(1)$ is the unit vector specifying the orientation of the dipole moment. Further, $c(12)$ in Eq. (44) is the direct correlation function of a bulk polar liquid depending on the positions and orientations of two molecules.[64] Somewhat distinct from this procedure, Calef and Wolynes[65] used the expansion of the density functional relative to the density $\rho_0(1)$ around the repulsive core of the solute. However,

in their approach, the reference direct correlation function $c(1,2)$ needs to include the effect of the solute core on the solvent structure. Establishing such a function is a complex problem on its own and the expansion used by Chandra and Bagchi[39] is preferable since it allows one to use $c(1,2)$ of the homogeneous liquid.

A. Total polarization density

The Gaussian functional that we are concerned with is obtained from Eq. (44) by expanding the logarithm in the first (ideal gas) term in the functional and keeping the terms up to the second order in $\delta\rho$.[39] One additionally expands both the microscopic density $\delta\rho(1)$ and $c(12)$ in rotational invariants.[66] The convolution present in the term containing the direct correlation function is converted into the integral by using the Fourier transform. The result is

$$\begin{aligned} F[\rho_k,\tilde{\mathbf{P}}] = &\frac{1}{2\beta\rho}\sum_{\mathbf{k}}\frac{|\rho_{\mathbf{k}}|^2}{S(k)} \\ &+\tfrac{1}{2}\sum_{\gamma,\mathbf{k}}\frac{|\tilde{\mathbf{P}}^{\gamma}|^2}{\chi^{\gamma}(k)}-\sum_{\mathbf{k}}\tilde{\mathbf{E}}_0\cdot(\tilde{\mathbf{P}}^{L}+\tilde{\mathbf{P}}^{T}). \end{aligned} \tag{45}$$

In this equation, $\rho_{\mathbf{k}}=\sum_j e^{i\mathbf{k}\cdot\mathbf{r}_j}$ is the density field and $S(k)=N^{-1}\langle|\rho_{\mathbf{k}}|^2\rangle$ is the density structure factor of the liquid.[64] The first summand thus describes Gaussian isotropic fluctuations of the liquid density, the sum over the reciprocal space is understood as the integral, $\sum_{\mathbf{k}}\to\int d\mathbf{k}/(2\pi)^3$. Further, $\tilde{\mathbf{P}}^{\gamma}$, $\gamma=\{\mathrm{L},\mathrm{T}\}$ specifies L and T projections of the dipolar polarization density in reciprocal space

$$\begin{aligned} \tilde{\mathbf{P}}^{L} &= \sum_j \hat{\mathbf{k}}(\mathbf{m}_j\cdot\hat{\mathbf{k}})e^{i\mathbf{k}\cdot\mathbf{r}_j}, \\ \tilde{\mathbf{P}}^{T} &= \sum_j \Big(\mathbf{m}_j-\hat{\mathbf{k}}(\mathbf{m}_j\cdot\hat{\mathbf{k}})\Big)e^{i\mathbf{k}\cdot\mathbf{r}_j}, \end{aligned} \tag{46}$$

where $\hat{\mathbf{k}}=\mathbf{k}/k$. We note that the formal expansion of the direct correlation function in rotational invariants produces the terms of the form $c^{101}(k)\rho_{\mathbf{k}}\tilde{\mathbf{P}}^{L}$, which can potentially couple the density and polarization fluctuations.[67] However, $\tilde{\mathbf{P}}^{L}$ and the entire expansion term alters its sign upon the simultaneous flip of all dipoles in the liquid. Since this symmetry operation cannot affect any observable property of the isotropic liquid, one has to require $c^{101}(k)=c^{011}(k)=0$. Therefore, polarization-density coupling does not appear in the quadratic (Gaussian) expansion of the density functional.[39]

The nonlocal susceptibilities $\chi^{\gamma}(k)$ in Eq. (45) are given by the fluctuation relations consistent with the Gaussian form of the polarization functional

$$\chi^{\gamma}(k)=\frac{\beta}{\Omega}\langle\delta\tilde{\mathbf{P}}^{\gamma}\cdot\delta\tilde{\mathbf{P}}^{\gamma *}\rangle, \tag{47}$$

where $\tilde{\mathbf{P}}^{\gamma *}$ denotes complex conjugate. The magnitude of the solvent dipole moment can be conveniently separated from the angular dipolar correlations expressed in terms of the dipolar orientational structure factors[35–37,68] through the relation $\chi^{\gamma}(k)=(3y/4\pi)S^{\gamma}(k)$. Here, the dipolar polarity parameter typically appearing in dielectric theories[28,29] is defined as

$$y=(4\pi/9)\beta\rho m^2. \tag{48}$$

Correspondingly, the dipolar structure factors involve only orientations $\hat{\mathbf{e}}_j=\mathbf{m}_j/m$ and positions $\mathbf{r}_j$ of the dipoles

$$\begin{aligned} S^{L}(k) &= \frac{3}{N}\sum_{i,j}(\hat{\mathbf{e}}_i\cdot\hat{\mathbf{k}})(\hat{\mathbf{k}}\cdot\hat{\mathbf{e}}_j)e^{i\mathbf{k}\cdot\mathbf{r}_{ij}}, \\ S^{T}(k) &= \frac{3}{2N}\sum_{i,j}\Big[\hat{\mathbf{e}}_i\cdot\hat{\mathbf{e}}_j-(\hat{\mathbf{e}}_i\cdot\hat{\mathbf{k}})(\hat{\mathbf{k}}\cdot\hat{\mathbf{e}}_j)\Big]e^{i\mathbf{k}\cdot\mathbf{r}_{ij}}. \end{aligned} \tag{49}$$

The second summand in Eq. (45) describes Gaussian fluctuations of the orthogonal longitudinal and transverse polarization fields. The last term gives the coupling of these fields to the Fourier transform of the electric field of the solute $\tilde{\mathbf{E}}_0$. The $k\to 0$ limit of this functional transforms into the Felderhof functional in Eq. (22). Correspondingly, the longitudinal and transverse susceptibilities used in the continuum polarization functionals are $k\to 0$ limits of the nonlocal functions, $\chi^{L,T}=\chi^{L,T}(0)$. There is obviously no ambiguity with the macroscopic limit $k\to 0$ when the functional of the overall polarization density $\tilde{\mathbf{P}}$ is concerned. This is not true anymore when the polarization field density is separated into the electronic and nuclear components. Before we proceed to that next step, one comment on the nature of the repulsive core potential introduced into the polar liquid by the solute is relevant here.

The Gaussian functional in Eq. (45) involves the long range electric field of the solute charges, but does not incorporate the solute-solvent repulsive potential. The reason was clarified by Chandler.[59] His Gaussian solvation model puts the repulsive potential as a separate constraint, applied to the Gaussian functional, of disappearing polarization field inside the repulsive core of the solute. This nonlinear condition, which obviously cannot be accommodated by simply adding the repulsive potential to the free energy functional, results in the renormalization of the Gaussian susceptibility functions. In the case of the polarization field, the problem can be formally solved in reciprocal space for the transverse and longitudinal projections of the polarization field.[45] The result is twofold: (i) the field of external (solute) charges is multiplied by the step function $\theta(\mathbf{r})$ equal to zero inside the repulsive core of the solute and (ii) the Gaussian susceptibilities $\chi^{\gamma}(k)$ get renormalized to functions $\chi^{\gamma}(\mathbf{k}_1,\mathbf{k}_2)$ depending on two wavevectors separately to reflect the inhomogeneous character of the problem. The Gaussian terms in Eq. (45) become 6D convolutions of fields $\mathbf{P}^{\gamma}$ with these inhomogeneous susceptibilities, instead of 3D summations based on the homogeneous susceptibilities $\chi^{\gamma}(k)$. In this article, we do not pursue this complete analysis of the problem and instead focus on the issue

of separating the the electronic and nuclear polarization fields in the solvent part of the free energy functional. Our focus is, therefore, primarily on the spectrum of fluctuations of these two fields in the bulk polar liquid.

B. Electronic and nuclear components

We now introduce two nonlocal reciprocal-space fields, $\tilde{\mathbf{P}}_e$ and $\tilde{\mathbf{P}}_n$, obtained by Fourier transform of the real-space fields $\mathbf{P}_e$ and $\mathbf{P}_n$. The extension is straightforward within the Chandra and Bagchi approach.[39] One needs to split $\delta\rho$ into the sum of $\delta\rho_e + \delta\rho_n$ and follow the same sequence of steps as used to arrive at the nonlocal functional in Eq. (45). One has to additionally assume that the direct correlation function includes both self-correlations between the $\delta\rho_{e,n}$ densities and the cross correlations between the electronic and nuclear components (see supplementary material for more detail[69]). Since the density field does not couple to the polarization field in the quadratic expansion, the final result can be given in the following compact form

$$F[\tilde{\mathbf{P}}_e, \tilde{\mathbf{P}}_n] = \tfrac{1}{2}\sum_{a,b}\sum_{\gamma,\mathbf{k}} \frac{\tilde{\mathbf{P}}_a^{\gamma}\cdot\tilde{\mathbf{P}}_b^{\gamma *}}{\alpha_{ab}^{\gamma}(k)} - \sum_{\mathbf{k}} \tilde{\mathbf{F}}_0\cdot(\tilde{\mathbf{P}}_e + \tilde{\mathbf{P}}_n), \tag{50}$$

where $\mathrm{a,b} = \mathrm{e,n}$ and $\gamma = \mathrm{L,T}$.

The functional in Eq. (50) employs a somewhat different notation scheme compared to the ones used in the literature and reviewed above. First, we have replaced the external field of charges $\tilde{\mathbf{E}}_0$ with an auxiliary field $\tilde{\mathbf{F}}_0$ to stress that we do not anticipate any specific symmetry of this field. It can carry either longitudinal or transverse character and is used here to probe either the longitudinal or transverse nuclear response of the polar-polarizable fluid. The field $\tilde{\mathbf{F}}_0$ also does not have to be associated with any, even imaginary, charge distribution,[43] that is one does not have to impose the restriction $\nabla\cdot\mathbf{F}_0 = 4\pi\rho_0$. Next, we have introduced double indexes $a, b = e, n$ in the nonlocal functions $\alpha_{ab}^{\gamma}(k)$ and switched from χ's for such functions to α's. This change in notations emphasizes that there are off-diagonal elements in the quadratic 2×2 matrix in the fields $\mathbf{P}_e$ and $\mathbf{P}_n$. In principle, the same notation scheme equally applies to the Lee-Hynes functional in Eq. (29), which also contains a cross "en" component linking the longitudinal projections of the polarization field. We used χ's there, with only one subscript, "e" or "n", for historical reasons.

In order to connect $\alpha_{ab}^{\gamma}(k)$ to properties available from simulations, they need to be related to susceptibility functions of the bulk polar liquid

$$\chi_{ab}^{\gamma}(k) = \frac{\beta}{\Omega}\langle \delta\tilde{\mathbf{P}}_a^{\gamma}\cdot\delta\tilde{\mathbf{P}}_b^{\gamma *}\rangle, \tag{51}$$

which are analogs of the longitudinal and transverse susceptibilities in Eq. (47), but involve separate electronic and nuclear polarization components. This connection is easy to establish and the result is

$$\begin{aligned} &\chi_{nn}^{\gamma} = \bar{\alpha}_n^{\gamma}, \quad \chi_{ee}^{\gamma} = (\alpha_{ee}^{\gamma}/\alpha_{nn}^{\gamma})\bar{\alpha}_n^{\gamma}, \\ &\chi_{en}^{\gamma} = -(\alpha_{ee}^{\gamma}/\alpha_{en}^{\gamma})\bar{\alpha}_n^{\gamma}, \end{aligned} \tag{52}$$

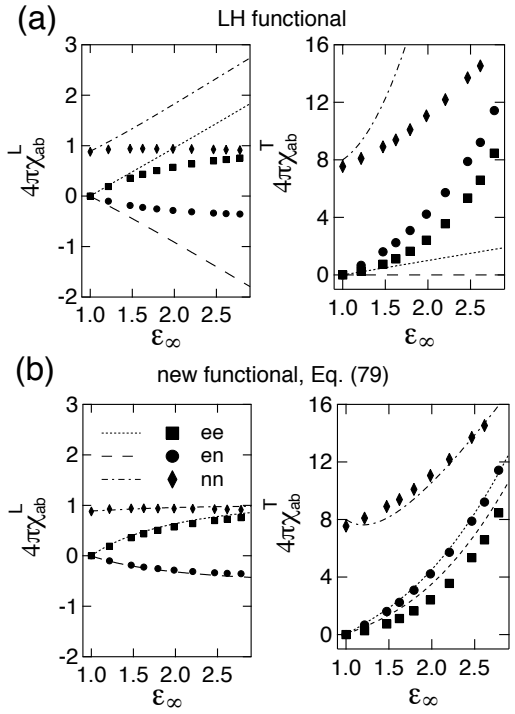

FIG. 5. Longitudinal (left column) and transverse (right column) χ_{ab}^{γ} calculated from MC simulations of polarizable hard spheres. The points are simulation results and the lines refer to the prediction from the Lee-Hynes functional ((a), Eq. (53)) and the present functional ((b), Eq. (79)). Shown are the components of χ_{ab}^{γ}: "ee" (squares and dotted lines), "en" (circles and dashed lines), and "nn" (diamonds and dash-dotted lines).

where $\bar{\alpha}_n^{\gamma} = \alpha_{nn}^{\gamma}/(1 - \alpha_{ee}^{\gamma}\alpha_{nn}^{\gamma}/(\alpha_{en}^{\gamma})^2)$ and we have dropped the dependence on k for brevity. These relations connect $\alpha_{ab}^{\gamma}(k)$ in the Gaussian functional to $\chi_{ab}^{\gamma}(k)$, which can be determined from computer simulations of polarizable liquids. The Lee-Hynes functional gives very specific predictions for the $k = 0$ values of these susceptibilities

$$\begin{aligned} &\chi_{ee}^{L} = \frac{(\epsilon_\infty - 1)(\epsilon_s - \epsilon_\infty + 1)}{4\pi\epsilon_s}, \quad \chi_{ee}^{T} = \frac{\epsilon_\infty - 1}{4\pi}, \\ &\chi_{en}^{L} = -\frac{(\epsilon_s - \epsilon_\infty)(\epsilon_\infty - 1)}{4\pi\epsilon_s}, \quad \chi_{en}^{T} = 0, \\ &\chi_{nn}^{L} = \frac{\epsilon_\infty(\epsilon_s - \epsilon_\infty)}{4\pi\epsilon_s}, \quad \chi_{nn}^{T} = \frac{\epsilon_s - \epsilon_\infty}{4\pi}. \end{aligned} \tag{53}$$

As is shown in Fig. 5, computer simulations do not support these functionalities for χ_{ab}^{γ}. We produce below an alternative set by extrapolating $\chi_{ab}^{\gamma}(k)$ from simulations to $k = 0$. Both sets are collected in Table I for direct comparison.

We can proceed from the general functional in Eq. (50) to eliminate the electronic polarization according to Eq.

TABLE I. Continuum susceptibilities χ^{γ}_{ab} ($a,b = e,n$ and $\gamma = L,T$) entering the Marcus/Lee-Hynes functional [Eq. (53)] and produced as the $k = 0$ extrapolation of $\chi^{\gamma}_{ab}(k)$ from numerical simulations in the present work [Eq. (79)].

ab	Marcus/Lee-Hynes		present work	
	L	T	L	T
ee	$\frac{(\epsilon_\infty-1)(\epsilon_s-\epsilon_\infty+1)}{4\pi\epsilon_s}$	$\frac{\epsilon_\infty-1}{4\pi}$	$\frac{(\epsilon_s-1)(\epsilon_\infty-1)}{3\pi\epsilon_s\epsilon_\infty}$	$\frac{(\epsilon_\infty-1)(\epsilon_s+2\epsilon_\infty)}{12\pi\epsilon_\infty}$
en	$-\frac{(\epsilon_s-\epsilon_\infty)(\epsilon_\infty-1)}{4\pi\epsilon_s}$	0	$-\frac{(\epsilon_s-1)(\epsilon_\infty-1)}{6\pi\epsilon_s\epsilon_\infty}$	$\frac{(\epsilon_s-\epsilon_\infty)(\epsilon_\infty-1)}{12\pi\epsilon_\infty}$
nn	$\frac{\epsilon_\infty(\epsilon_s-\epsilon_\infty)}{4\pi\epsilon_s}$	$\frac{\epsilon_s-\epsilon_\infty}{4\pi}$	$\frac{\epsilon_s-1}{4\pi\epsilon_s}$	$\frac{\epsilon_s-\epsilon_\infty}{4\pi\epsilon_\infty}$

(35) or by direct minimization with respect to $\tilde{\mathbf{P}}^{\gamma}_e$. Either approach results in the non-equilibrium functional of the nuclear polarization field

$$E[\tilde{\mathbf{P}}_n] = F_e + \tfrac{1}{2}\sum_{\gamma,\mathbf{k}} \frac{|\tilde{\mathbf{P}}^{\gamma}_n|^2}{\chi^{\gamma}_{nn}(k)} - \sum_{\gamma,\mathbf{k}} q^{\gamma}(k)\tilde{\mathbf{F}}^{\gamma}_0\cdot\tilde{\mathbf{P}}^{\gamma}_n, \quad (54)$$

where the screening function is

$$q^{\gamma}(k) = 1 + \chi^{\gamma}_{en}(k)/\chi^{\gamma}_{nn}(k). \quad (55)$$

By comparing Eq. (54) to Eq. (41), one observes that the screening factor q in Eq. (41) becomes a nonlocal function $q^{\gamma}(k)$ in the microscopic formulation. In addition, the susceptibility of the nuclear fluctuations $\chi^{\gamma}_{nn} = \bar{\alpha}^{\gamma}_n$ is re-normalized by coupling between the permanent and induced dipoles, which is a microscopic analog of the dipole-dipole screening factor p in Eq. (41). We also note that F_{0e} in Eq. (54) is determined in terms of the susceptibility functions $\alpha^{\gamma}_{ee}(k)$ instead of $\chi^{\gamma}_{ee}(k)$

$$F_e = -\tfrac{1}{2}\sum_{\gamma,\mathbf{k}} \alpha^{\gamma}_{ee}|\tilde{\mathbf{F}}^{\gamma}_0|^2. \quad (56)$$

A connection to χ^{γ}_{ab} can be established through Eq. (52).

Equation (54) is the general result for the microscopic functional describing the electronic system in equilibrium with the electronic polarization of the medium, but subjected to a non-equilibrium fluctuation of the nuclear polarization. Two approximations are involved in arriving at this general form: the second-order expansion of the ideal gas term of the Chandra-Bagchi functional[39] and truncation of the expansion of $c(12)$ in rotational invariants after the first two expansion terms. The latter assumption is exact for purely dipolar fluids, but becomes approximate for general multipolar fluids.[66] Within these limitations, defining the screening functions $q^{\gamma}(k)$ and the susceptibilities $\chi^{\gamma}_{nn}(k)$ fully resolves the problem. Below, we gain access to these functions from atomistic simulations. These results can then be applied back to remap the standard continuum functionals (see below).

The longitudinal continuum susceptibility of electron transfer theories appears in the continuum limit $k \to 0$ taken in the nonlocal functions and the common approximation of the longitudinal external field $\tilde{\mathbf{F}}_0 = \tilde{\mathbf{F}}^{L}_0$. One arrives at the reorganization energy in Eq. (4) with the longitudinal susceptibility defined as

$$\chi^{L}_m = \chi^{L}_{nn}(q^L)^2, \quad (57)$$

where $q^L = q^L(0)$ and $\chi^{L}_{ab} = \chi^{L}_{ab}(0)$. This continuum susceptibility obtained from simulations is shown by open points in Fig. 2.

IV. Numerical simulations

A. Simulation protocol

Two families of polarizable fluids were used here to produce nonlocal susceptibilities in reciprocal space. We simulated a series of polarizable hard-sphere fluids following the protocol developed in Ref. 31 and a number of force-field fluids with varying polarizability based on the polarizable SWM4-DP water.[70] Statistical configurations are produced by the Monte Carlo (MC) protocol for the polaraizable hard spheres and by molecular dynamics (MD) for polarizable water, for which NAMD[71] was used. Both types of systems model molecular polarizability by a Drude induced dipole, adjusted to the local instantaneous field according to the molecular polarizability.

The simulation protocol is somewhat more complex than standard simulations of polar liquids[35,72] since one has to distinguish between dipolar correlations arising from permanent and induced dipoles. Their magnitudes are not equal and, in addition, the induced dipoles fluctuate in response to fluctuating local fields. The Hamiltonian of the liquid is that of classical Drude oscillators describing fluctuating induced dipoles $\mathbf{p}_j$ characterized by isotropic polarizability α

$$U = U_{\rm HS} - \tfrac{1}{2}\sum_{i\neq j}(\mathbf{m}_i+\mathbf{p}_i)\cdot\mathbf{T}_{ij}\cdot(\mathbf{m}_j+\mathbf{p}_j) + \sum_j \frac{p_j^2}{2\alpha}, \quad (58)$$

where $U_{\rm HS}$ is the repulsive potential between the molecules, which is the hard-sphere repulsion for polarizable spheres. The latter approximation reduces the number of parameters characterizing the thermodynamic state of the liquid to just three dimensionless parameters:

$(m^*)^2 = \beta m^2/\sigma^3$, $\rho^* = \rho\sigma^3$, and $\alpha^* = \alpha/\sigma^3$ (σ is the hard-sphere diameter).

From Eq. (58), the induced dipole in equilibrium with the instantaneous electric field of the permanent dipoles

$$\mathbf{E}_i = \sum_k \mathbf{T}_{ij} \cdot \mathbf{m}_j \tag{59}$$

can be found by the inversion of the matrix equation

$$\sum_j \mathbf{B}_{ij} \cdot \bar{\mathbf{p}}_j = \alpha \mathbf{E}_i, \tag{60}$$

where $\mathbf{B}_{ij}$ is a 3×3 matrix

$$\mathbf{B}_{ij} = \mathbf{I}\delta_{ij} - \alpha \mathbf{T}_{ij}. \tag{61}$$

The manifold of $\mathbf{B}_{ij}$ matrices for all $i, j = 1, \ldots, N$ makes a $3N \times 3N$ matrix $\mathbf{B}$, which needs to be inverted at each nuclear configuration to obtain the set of induced dipoles $\bar{\mathbf{p}}_i$.[73]

Instead of the matrix inversion, our simulation protocol implemented in the MPI-parallelized package MCPOL[74] employed the iterative scheme of Vesely.[75] Each induced dipole within the cutoff sphere is updated according to the rule $\bar{\mathbf{p}}_k = \alpha \bar{\mathbf{E}}_k(\mathbf{p}_1, \ldots, \mathbf{p}_M)$, where $\bar{\mathbf{E}}_k$ is the total electric field of both permanent and induced dipoles at the location of particle k. Since the electric field depends on all M induced dipoles within the cutoff radius, each update is used to re-calculate the field until the change of the induced dipole does not exceed a given error margin. Typically 3-5 iterations for all dipoles within the cutoff sphere are required following each MC move, involving either a center-of-mass translation or a dipole rotation, to reach the relative error of 10^{-5} for the field magnitude. The dipolar interactions were truncated with the reaction-field correction[31,76] for $N = 864$ particles in the cubic simulation box with the side length L replicated with the periodic boundary conditions. Each MC move was followed by an update of the induced dipoles within the cutoff sphere of the radius $r_p/L = 0.5$. The total of 5×10^5 MC cycles including all particles in the box were done for each polarizable fluid. The calculations of the susceptibility functions were corrected for finite-size effects according to Neumann[77] and, after the correction, were extrapolated to $k = 0$ to obtain the dielectric constants corresponding to a macroscopic sample (see supplementary material[69] for more details and examples of calculations).

A slightly different protocol accounting for water polarizability is used in MD simulations. A separate Drude particle, carrying the charge q_D and the mass m_D is attached to the molecule through a harmonic spring with a force constant k_D. Its trajectory is separately calculated within the MD run of the system. Any fluctuations of the Drude particle comes as a violation of the Born-Oppenheimer approximation and need to be avoided. This is achieved in NAMD[71] by both using a small mass m_D and a low temperature of a separate thermostat used for Drude particles.[78] The temperature $T^* \simeq 1$ K is chosen to leave almost no kinetic energy to the Drude-atom vibrations, but still to allow them to adjust to the local field with the isotropic polarizability $\alpha = q_D^2/k_D$. One, therefore, produces the induced dipoles $\bar{\mathbf{p}}_k$ along the MD trajectory with small fluctuations consistent with the temperature T^*.[70] More details of the simulation protocols and data analysis are given in the supplementary material.[69] We now turn to the results.

B. Susceptibilities and structure factors

The dipolar susceptibilities for induced and permanent dipoles and their cross terms are given by Eq. (51). The overall susceptibility, corresponding to the variance of the longitudinal or transverse projection of the total (permanent plus induced) dipole moment, is given in terms of components as follows

$$\chi^\gamma(k) = \chi^\gamma_{nn}(k) + \chi^\gamma_{ee}(k) + 2\chi^\gamma_{en}(k). \tag{62}$$

In addition to susceptibilities, it is convenient to introduce structure factors of dipolar polarization,[64,79] which are based on unit vectors of dipolar orientations instead of the dipole moments. Such definitions are straightforward for one-component dipolar liquids [Eq. (49)], but are more limited in the case of fluctuating induced dipoles. We, therefore, normalize the structure factors based on the magnitude of the permanent dipoles according to the relation

$$\chi^\gamma_{ab} = \frac{3y}{4\pi} S^\gamma_{ab}, \tag{63}$$

where y is given by Eq. (48). For the component related to permanent dipoles, $\chi^\gamma_{nn}(k)$ provides the standard connection to the structure factors in Eq. (49). According to this definition, the induced dipoles are normalized in the structure factor by the magnitude of the permanent dipole. One gets for the longitudinal component

$$S^L_{ee} = \frac{3}{Nm^2} \sum_{i,j} \left\langle (\mathbf{p}_i \cdot \hat{\mathbf{k}})(\hat{\mathbf{k}} \cdot \mathbf{p}_j) e^{i\mathbf{k}\cdot\mathbf{r}_{ij}} \right\rangle. \tag{64}$$

The transverse component is constructed similarly to Eq. (49). The cross structure factor is obtained by replacing $\mathbf{p}_j/m \to \hat{\mathbf{e}}_j$ in the above equation.

The simulation protocol outlined above generates a sequence of equilibrium induced dipoles $\bar{\mathbf{p}}_j(n) = \alpha \mathbf{E}_j(n)$ at each step of the trajectory n. Therefore, $\bar{\mathbf{p}}_j$ is not the fluctuating variable $\mathbf{p}_j$ in Eq. (64) and an additional step is required to make the statistical average consistent with the nuclear configurations produced by the simulation protocol. We first introduce the rank two tensor

$$Z^{\alpha\beta}_{ij} = \langle p^\alpha_i p^\beta_j e^{i\mathbf{k}\cdot\mathbf{r}_{ij}} \rangle, \tag{65}$$

where α, β denote the Cartesian projections and the average is taken over both the positions of the dipoles and the fluctuations of the Drude induced dipoles

$$\langle \ldots \rangle = Q^{-1} \int \ldots e^{-\beta U} \prod_k d\mathbf{p}_k d\mathbf{r}_k \tag{66}$$

and Q is the partition function. The average in Eq. (65) can be conveniently re-written in terms of an auxiliary field $\mathbf{A}_j$

$$Z_{ij}^{\alpha\beta} = \frac{\partial}{\partial A_i^\alpha}\frac{\partial}{\partial A_j^\beta}\Big\langle e^{i\mathbf{k}\cdot\mathbf{r}_{ij}+\sum_i \mathbf{A}_i\cdot\mathbf{p}_i}\Big\rangle\Big|_{\mathbf{A}_i=0}. \tag{67}$$

From Eqs. (66) and (67) one derives the expression for the structure factor of the induced dipoles

$$S_{ee}^L(k) = \frac{3}{Nm^2}\sum_{i,j} \Big\langle e^{i\mathbf{k}\cdot\mathbf{r}_{ij}}\left[\frac{\alpha}{\beta}\hat{\mathbf{k}}\hat{\mathbf{k}}{:}(\mathbf{B}^{-1})_{ij} + (\bar{\mathbf{p}}_i\cdot\hat{\mathbf{k}})(\hat{\mathbf{k}}\cdot\bar{\mathbf{p}}_j)\right]\Big\rangle_{\rm sim}, \tag{68}$$

where $\hat{\mathbf{k}}\hat{\mathbf{k}}{:}(\mathbf{B}^{-1})_{ij} = k_\alpha k_\beta (B^{-1})_{ij}^{\alpha\beta}$. In this equation, the induced dipoles $\bar{\mathbf{p}}_i$ in equilibrium with the local field are directly produced by the simulation protocol and the inverted matrices $(\mathbf{B}^{-1})_{ij}$ [Eq. (61)] are calculated at each simulation configuration. The average $\langle\ldots\rangle_{\rm sim}$ in this equation includes only nuclear motions (translations and rotations), but does not include fluctuations of the magnitude of the induced dipole included in Eq. (64). Since $\langle\delta\mathbf{p}_j\rangle = 0$, matrix inversion is not required for the cross, electronic-nuclear, structure factors. They are calculated from the induced dipoles $\bar{\mathbf{p}}_i$ and unit vectors of the permanent dipoles $\hat{\mathbf{e}}_j$

$$S_{en}^L(k) = \frac{3}{Nm}\sum_{i,j}\Big\langle e^{i\mathbf{k}\cdot\mathbf{r}_{ij}}(\bar{\mathbf{p}}_i\cdot\hat{\mathbf{k}})(\hat{\mathbf{k}}\cdot\hat{\mathbf{e}}_j)\Big\rangle_{\rm sim}. \tag{69}$$

Similar expressions can be written for the transverse structure factors $S_{ab}^T(k)$.

The limit of large wavevector magnitudes $k\sigma \gg 1$ is easy to establish for all structure factors given that correlations between different dipoles vanish in this limit. One therefore obtains the following asymptotes

$$\begin{aligned} &S_{nn}^\gamma \to 1,\\ &S_{ee}^\gamma \to y_{\rm ind}/y,\\ &S_{en}^\gamma \to \frac{y_{\rm eff}-y_{\rm ind}}{2y} - \frac{1}{2}. \end{aligned} \tag{70}$$

Here, the polarity parameter of the induced dipoles is

$$\frac{y_{\rm ind}}{y} = \frac{\langle\bar{p}^2\rangle}{m^2} + \frac{\alpha}{\beta m^2}\langle(B^{-1})^{\alpha\alpha}\rangle, \tag{71}$$

where summation over the common Cartesian indexes is assumed. Correspondingly, the effective polarity parameter is given as

$$\frac{y_{\rm eff}}{y} = 1 + \frac{y_{\rm ind}}{y} + \frac{2}{m}\langle\hat{\mathbf{e}}\cdot\bar{\mathbf{p}}\rangle. \tag{72}$$

Figure 6 shows an example of structure factors calculated for the polarizable hard spheres at $\alpha^* = 0.02$ and the corresponding $k\sigma \gg 1$ limits (thick dashed lines), which are satisfied in our calculations.

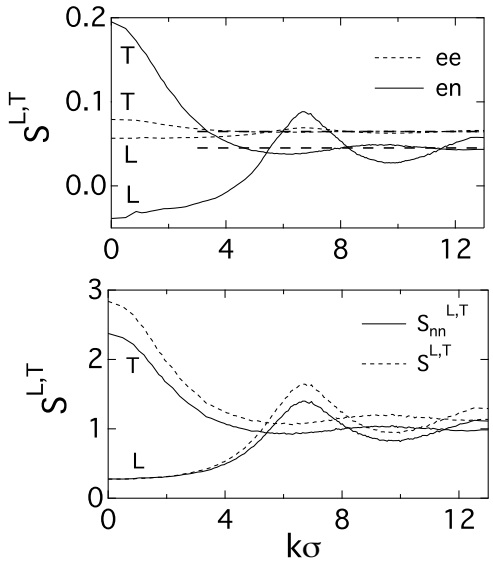

FIG. 6. Components of the total structure factors $S^{L,T}(k)$. The thick dashed lines in the upper panel show the asymptotic limits of "ee" and "en" components at $k\sigma \gg 1$ [Eq. (70)]. The $k = 0$ values of the structure factors are obtained by extrapolating the linear dependence of $(S_{ab}^{L,T}(k))^{-1}$ vs k^2 to $k = 0$. The results are obtained by MC simulations of a polarizable hard-sphere fluid with $(m^*)^2 = 1.0$, $\rho^* = 0.8$, $\alpha^* = 0.02$ ($\epsilon_\infty = 1.27$), and $N = 864$ particles in the cubic simulation box.

There are no obvious solutions for the $k = 0$ values of the structure factors. The smallest values of $k\sigma$ available from our simulations are 0.866 (polarizable hard spheres) and 0.62 (polarizable water, for which the effective hard-sphere diameter $\sigma = 2.87$ Å was adopted[80]). The $k = 0$ values of the structure factors were obtained from extrapolating the finite-size simulation results. The procedure is based on the expansion of the direct correlation function at small k:[64,66,79] $c(k) = c(0) + c_2k^2$. From this equation, and the Fourier transformed form of the Ornstein-Zernike equation, the inverse structure factors should change as linear functions of k^2 at $k\sigma \ll 1$. Their $k = 0$ values were therefore obtained as $k = 0$ intercepts of the linear plots of $(S_{ab}^{L,T}(k))^{-1}$ vs k^2 (Fig. S4 in the supplementary material[69]).

The connection of the susceptibilities $\chi^\gamma = \chi^\gamma(0)$ in Eq. (62) to the results of the dielectric experiment deserves careful consideration. We first notice that the polarization density field $\mathbf{P}$ and its Fourier transform $\tilde{\mathbf{P}}$ absorbs into itself all components involving the molecular polarizability. The equilibrium field $\mathbf{P}_e^{\rm eq}$, obtained by minimizing both local and nonlocal functionals, is in equilibrium with the field of external charges and with the instantaneous nuclear polarization field $\mathbf{P}_n$.[23,25] This

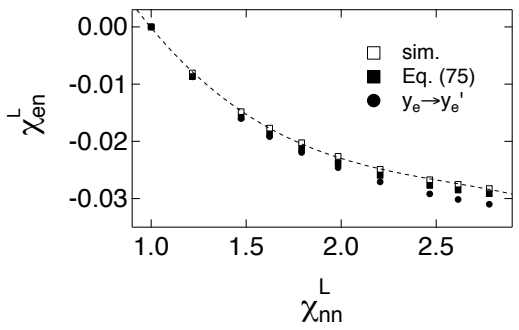

FIG. 7. $\chi^L_{en}(0)$ vs $\chi^L_{nn}(0)$ calculated from simulations (sim., open squares) and from Eq. (75) (filled squares). The filled circles show the use of y'_e instead of y_e in Eq. (75). The dashed line is a regression drawn through the simulation points to guide the eye.

partitioning of the polarization field, known in the literature as the Marcus partitioning,[18,81] is the best physically motivated approach to the problem both from the viewpoint of constructing the polarization functional and from the viewpoint of performing numerical simulations. Consistent with this definition, the susceptibilities χ^γ_{ee} and the structure factors S^γ_{ee} include all components related to molecular polarizability, i.e., both the induced dipoles $\bar{\mathbf{p}}_k$ in equilibrium with the instantaneous local field and Drude fluctuating dipoles $\delta\mathbf{p}_k = \mathbf{p}_k - \bar{\mathbf{p}}_k$. However, only the latter component is probed by the high-frequency dielectric experiment, which leaves $\bar{\mathbf{p}}_j$ dynamically frozen on the time-scale ω_f^{-1}. Therefore, ϵ_∞ is associated with the second summand in Eq. (71). More specifically, one defines the condensed-phase high-frequency polarity parameter

$$y'_e = (4\pi/9)\rho\alpha\langle(B^{-1})^{\alpha\alpha}\rangle, \tag{73}$$

which corresponds to the condensed-phase renormalized molecular polarizability appearing in mean-field theories of polar liquids.[28,82] This parameter should be used instead of y_e in the Clausius-Mossotti equation, Eq. (43) with $\Theta = 0$. Given these specifics, we cannot directly identify χ^γ_{ee} with ϵ_∞, but can link the total susceptibilities to the static dielectric constant ϵ_s

$$\chi^L = \frac{\epsilon_s - 1}{4\pi\epsilon_s}, \quad \chi^T = \frac{\epsilon_s - 1}{4\pi}. \tag{74}$$

The trace of the total susceptibility $\chi^L + 2\chi^T$ yields the Onsager-Kirkwood expression in Eq. (27). The Pekar factor, $\chi^L_P = \chi^L - \chi^L_e$, is calculated from simulations by combining χ^L from Eq. (74) with χ^L_e is from Eq. (1), where y'_e from simulations is used in the Clausius-Mossotti equation to calculate ϵ_∞. This calculation is shown by filled points in Fig. 2.

Figure 6 shows that the longitudinal cross susceptibility between the induced and permanent dipoles, and the corresponding structure factor $S^L_{en}(k)$, are negative at $k \to 0$. In the longitudinal response, the oscillatory $\exp(i\mathbf{k}\cdot\mathbf{r}_{ij})$ phase factor eliminates the contributions to dipolar correlations from head-to-tail dipoles and enhances the effect of dipoles in the direction perpendicular to the orientation of a given target dipole.[29] Those equatorial dipoles tend to orient oppositely to a target permanent dipole and thus produce an induced dipole oriented oppositely to the target dipole. This is the origin of the negative values of $S^L_{en}(0)$ and $\chi^L_{en}(0)$. The opposite effect is observed for the transverse response (Fig. 6) since tail-to-head dipoles dominate in that case.

This general physical picture is well captured by the mathematical form suggested by Madden and Kivelson in their microscopic derivation of the Clausius-Mossotti equations. The connection between $\chi^L_{en}(k)$ and $\chi^L_{nn}(k)$ is given in their formalism (Eqs. (9.10) and (9.14) in Ref. 29) as

$$\chi^L_{en}(k) = -\frac{2y_e}{1+2y_e}\chi^L_{nn}(k), \tag{75}$$

where y_e is the polarizability density in Eq. (10). This relation is an approximation. However, since the formalism of diagram summation based on it leads to the Clausius-Mossotti equation,[29] which typically performs well for dense liquids, it is expected to be accurate as well. We indeed find it to reproduce exceptionally well the relation between χ^L_{en} and χ^L_{nn} from numerical simulations (Fig. 7).

Figure 7 shows that the use of y_e, instead of y'_e in Eq. (75) is more consistent with simulations. It is still convenient to provide a result for χ^L_m based on ϵ_∞, which requires y'_e. Since the distinction between using y_e and y'_e in Eq. (75) is not significant, we find from Eq. (57)

$$\chi^L_m = \chi^L_{nn}\left(\frac{\epsilon_\infty + 2}{3\epsilon_\infty}\right)^2. \tag{76}$$

The susceptibility χ^L_{nn} is not directly related to the dielectric constants. We, however, find from our simulations that, within simulations uncertainties, $\chi^L_{nn} \simeq \chi^L$. Therefore, from Eqs. (74) and (76), one arrives at a simple alternative to the standard Pekar susceptibility given by Eq. (8). Note also that from Eqs. (55) and (75) the $k = 0$ value of the screening function $q^L(0)$ is equal to q at $\Theta = 0$ in Eq. (42). As mentioned above, this is an expected outcome since $\Theta = 0$ leads to the Clausius-Mossotti result in Eq. (43).

For the transverse susceptibility, we find empirically $\chi^T_{nn} \simeq (\epsilon_s - \epsilon_\infty)/(4\pi\epsilon_\infty)$ and, from the equation presented by Madden and Kivelson for the transverse component,[29] the equation for the cross susceptiblity

$$\chi^T_{en} = \frac{(\epsilon_s - \epsilon_\infty)(\epsilon_\infty - 1)}{12\pi\epsilon_\infty}. \tag{77}$$

The comparison of this equation to simulations is shown in Fig. S5 in supplementary material.[69] As expected, from the arguments presented above, the transverse cross

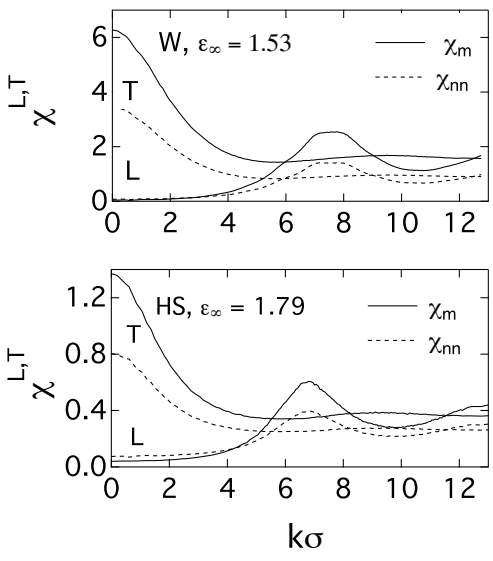

FIG. 8. Nuclear solvation susceptibility $\chi_m^\gamma(k)$, $\gamma = L, T$ as defined by Eq. (81) (solid lines) and the bare susceptibility $\chi_{nn}^\gamma(k)$ given by Eq. (63) (dashed lines). The results are shown for SWM4-DP water (W, upper panel) with $\epsilon_\infty = 1.53$ and for the fluid of polarizable hard spheres with $\alpha^* = 0.06$ and $\epsilon_\infty = 1.79$ (HS, lower panel).

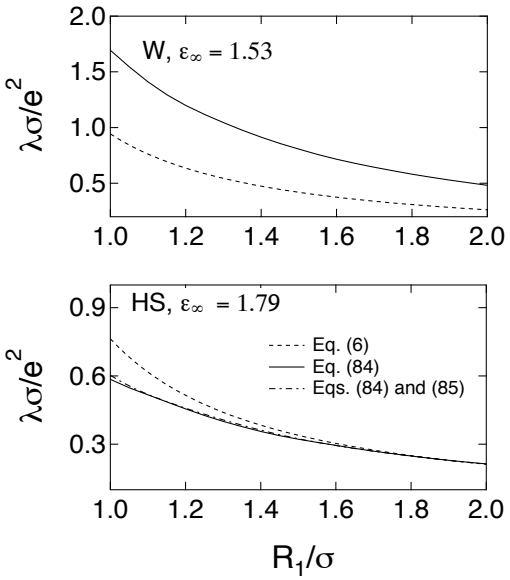

FIG. 9. Reorganization energy of electron transfer in the two-sphere Marcus configuration characterized by the donor and acceptor of equal radii R_d separated by the distance R. The solid lines show the calculation done through integration in reciprocal space [Eq. (84)] with the nuclear susceptibility $\chi_m^L(k)$ obtained from numerical simulations according to Eq. (81). The dashed line represents the Marcus formula (Eq. (6)), which is obtained from the integral in Eq. (84) by replacing $\chi_m^L(k) \to \chi_P^L$ and $R_1 \to R_d$. The upper panel shows the results of MD for SWM4-DP water (W) with $\epsilon_\infty = 1.53$, $\epsilon_s = 81$, and $\sigma = 2.87$ Å.[80] The lower panel shows the results of MC simulations for the fluid of polarizable hard spheres (HS) with $\alpha^* = 0.06$, $\epsilon_s = 19$, and $\epsilon_\infty = 1.79$. The dash-dotted line in the lower panel, almost indistinguishable on the scale of the plot from the solid line, refers to the result of integration in Eq. (84) with the approximate nonlocal longitudinal susceptibility given by Eq. (85).

susceptibility is positive at $k = 0$ (Fig. 6). We therefore obtain the transverse analog of Eq. (8)

$$\chi_m^T = \frac{\epsilon_s - \epsilon_\infty}{4\pi\epsilon_\infty}\left(\frac{\epsilon_\infty + 2}{3}\right)^2. \tag{78}$$

To summarize, our results suggest that the susceptibilities in the Lee-Hynes functional listed in Eq. (53) should be replaces by the following set consistent with the simulations

$$\begin{aligned}
&\chi_{ee}^L = \frac{(\epsilon_s - 1)(\epsilon_\infty - 1)}{3\pi\epsilon_s\epsilon_\infty}, \quad \chi_{ee}^T = \frac{(\epsilon_\infty - 1)(\epsilon_s + 2\epsilon_\infty)}{12\pi\epsilon_\infty},\\
&\chi_{en}^L = -\frac{(\epsilon_s - 1)(\epsilon_\infty - 1)}{6\pi\epsilon_s\epsilon_\infty}, \quad \chi_{en}^T = \frac{(\epsilon_s - \epsilon_\infty)(\epsilon_\infty - 1)}{12\pi\epsilon_\infty},\\
&\chi_{nn}^L = \frac{\epsilon_s - 1}{4\pi\epsilon_s}, \quad \chi_{nn}^T = \frac{\epsilon_s - \epsilon_\infty}{4\pi\epsilon_\infty}.
\end{aligned} \tag{79}$$

The comparison of these functionalities to numerical simulations is shown by Fig. 5. These equations are listed alongside those used in the Lee-Hynes functional in Table I. This set of susceptibilities applies to the continuum functional and does not fully resolve the problem of free energy calculations. Full nonlocal susceptibilities, depending on the wavevector, are essential for many practical situations as we show next.

V. Longitudinal reorganization energy

Here we present the calculation of the reorganization energy in terms of the effective nonlocal nuclear susceptibility. Because of the difficulties of dealing with transverse field components discussed above,[83] we limit ourselves here with the longitudinal fields. The corresponding free energy of nuclear solvation (Fig. 1) becomes (see Eq. (15))

$$F_n = -\tfrac{1}{2}\chi_m^L(k) * |\tilde{\mathbf{F}}_0^L|^2, \tag{80}$$

where, similarly to Eqs. (55) and (57), one has

$$\chi_m^\gamma(k) = \chi_{nn}^\gamma(k)(1 + \chi_{en}^\gamma(k)/\chi_{nn}^\gamma(k))^2. \tag{81}$$

The comparison of $\chi_m^\gamma(k)$ to $\chi_{nn}^\gamma(k)$ is shown in Fig. 8.

From Eq. (80), the reorganization energy becomes

$$\lambda = \tfrac{1}{2}\chi_m^L(k) * |\Delta\tilde{\mathbf{E}}_0^L|^2. \tag{82}$$

where $\Delta\tilde{\mathbf{E}}_0^L$ is the longitudinal field of the electron transfer dipole. In the two-sphere Marcus configuration, in which ones considers the donor and acceptor as two

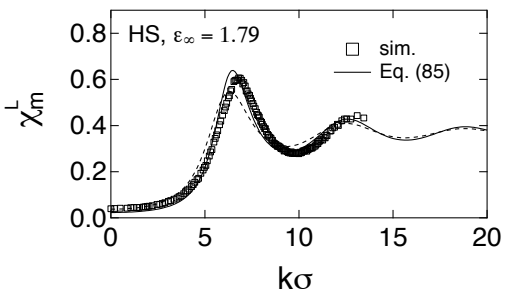

FIG. 10. $\chi_m^L(k)$ from simulations (sim., points) and from Eq. (85) (lines). The longitudinal polarity parameter $\xi^L = 0.17$ in $S_B(k, 2\xi^L)$ is adjusted to achieve the best fit of the simulation results obtained for polarizable hard spheres (HS) with $(m^*)^2 = 1.0$, $\rho^* = 0.8$, $\alpha^* = 0.06$, and $\epsilon_\infty = 1.79$. The dashed line is calculated from Eq. (85) with ξ^L from Eq. (87).

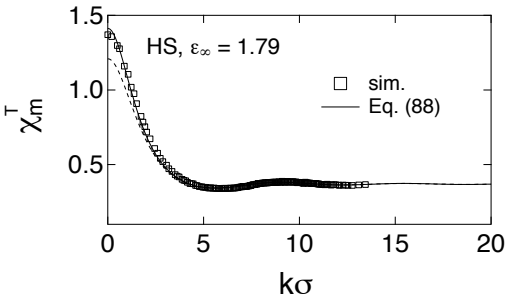

FIG. 11. $\chi_m^T(k)$ from simulations (sim., points) and from Eq. (88) (line). The solid line is the best fit to Eq. (88), the dashed line uses ξ^T from Eq. (89). The simulation results are for polarizable hard spheres (HS) with $(m^*)^2 = 1.0$, $\rho^* = 0.8$, $\alpha^* = 0.06$, and $\epsilon_\infty = 1.79$.

spheres with equal radii R_d separated by the distance $R \geq 2R_d$, one has[84]

$$\Delta\tilde{\mathbf{E}}_0^L = \frac{4\pi i e\mathbf{k}}{k^2} j_0(kR_1)\left[1 - e^{i\mathbf{k}\cdot\mathbf{R}}\right], \tag{83}$$

where $j_n(x)$ is a spherical Bessel function, e is the elementary charge, and the solvent-excluded radius $R_1 = R_d + \sigma/2$ has to be used in microscopic theories involving finite size of the solvent molecules characterized by the hard-sphere diameter σ. Our cavity is thus defined by the solvent-accessible surface, with $\sigma = 2.87$ Å,[80] also adopted in calculations with the polarizable water. The consistent transition from microscopic to continuum theories is achieved by shrinking the solvent size to zero ($\sigma \to 0$). Since the nonlocal susceptibilities are in fact functions of $k\sigma$, this limit also implies taking the $k \to 0$ limit in all susceptibility functions.[84]

The use of Eq. (83) in Eq. (82) results in the numerical integral which can be evaluated with the susceptibility $\chi_m^L(k)$ obtained from simulations

$$\lambda = 8e^2 \int_0^\infty j_0(kR_1)^2 \left[1 - j_0(kR)\right] \chi_m^L(k) dk. \tag{84}$$

Upon applying the continuum limit $\chi_m^L(k) = \chi_P^L = c_0/(4\pi)$ and replacing R_1 with R_d, the above equation reduces to the Marcus formula in Eq. (6).

Figure 9 compares the results of direct integration in Eq. (84) with the continuum Marcus formula in Eq. (6). The results are close for this specific polarizability, which corresponds to nearly crossing of the continuum and microscopic reorganization energies plotted against ϵ_∞ in Fig. 3. The overall dependence on ϵ_∞ is, however, different in two approaches. Since the continuum limit of the microscopic susceptibility is consistent with the Pekar result (Fig. 2), the difference in the dependence on ϵ_∞ arises from the nonlocal character of the dipolar nuclear response which cannot be neglected.

An analytic expression for $\chi_m^L(k)$ reproducing simulations can be derived from the Wertheim solution for the fluid of dipolar hard spheres.[62] It casts the dipolar structure factor in the form of Baxter's solution of the Percus-Yevick closure for a hard-sphere fluid.[64] In order to use this solution for our purposes, the $k = 0$ and $k \to \infty$ limits of $\chi_m^L(k)$ need to be satisfied. This is achieved by representing $\chi_m^L(k)$ in the form

$$\chi_m^L(k) = \chi_m(\infty) S_B(k, 2\xi^L), \tag{85}$$

where

$$\chi_m(\infty) = \frac{3y}{16\pi}\left(1 + \frac{y_{\text{eff}} - y_{\text{ind}}}{y}\right)^2 \tag{86}$$

follows from Eq. (70). Note that $\chi_m^L(\infty) = \chi_m^T(\infty) = \chi_m(\infty)$.

The Baxter function[62,64] $S_B(k, 2\xi^L)$ (see supplementary material for more detail[69]) depends on the longitudinal polarity parameter ξ^L, which can be adjusted to fit $\chi_m^L(k)$ (solid line in Fig. 10). Alternatively, ξ^L can be set by requiring to reproduce $\chi_m^L = \chi_m^L(0)$. This requirement results in the following relation for ξ^L

$$\frac{(1 - 2\xi^L)^4}{(1 + 4\xi^L)^2} = \frac{\chi_m^L}{\chi_m(\infty)}, \tag{87}$$

where χ_m^L is given by Eq. (8). The longitudinal nuclear susceptibility with such defined polarity parameter is shown by the dashed line in Fig. 10. While this parameterization somewhat misses the position of the peak of $\chi_m^L(k)$, it still yields a reliable result for λ in Eq. (84) (dash-double-dotted line in Fig. 9). We also note that the use of this type of parameterization for fitting $\chi_m^L(k)$ for water requires a scaling parameter in front of k because water has a more open structure than hard-sphere fluids.[32] A corresponding fit is shown by Fig. S8 in supplementary material.[69]

While we do not use the transverse nuclear susceptibility in the calculations of the reorganization energy

presented here, this function is required in the calculations involving complex shapes of the donor-acceptor complex.[83] The transverse nuclear susceptibility is given by the equation similar to Eq. (85)

$$\chi_m^T(k) = \chi_m(\infty) S_B(k, -\xi^T), \tag{88}$$

where the transverse structure factor is given by the Baxter function $S_B(k, -\xi^T)$. Similarly to the longitudinal response, ξ^T can be determined by requiring to reproduce χ_m^T in Eq. (78)

$$\frac{(1+\xi^T)^4}{(1-2\xi^T)^2} = \frac{\chi_m^T}{\chi_m(\infty)}. \tag{89}$$

This route is less satisfactory in comparison to the simulation results (dashed line) than direct fitting (solid line, Fig. 11) because of a somewhat underestimated χ_m^T produced by Eq. (78) (Fig. S8 in supplementary material[69]).

Equations (85)–(87) provide a closed solution for the longitudinal solvation susceptibility, which can be applied to the calculation of the longitudinal reorganization energy by k-space integration in Eq. (84).[85] One needs ϵ_s, ϵ_∞, σ (hard-sphere diameter),[80] m (dipole moment), and ρ (number density) as parameters of the solvent. The only parameter not directly provided by standard tabulation of solvent properties is the effective polarity of polar-polarizable liquids y_{eff} (see Table S1 in supplementary material[69] for the values obtained in simulations). This parameter is usually written[28] in terms of the effective condensed-matter dipole moment m'

$$y_{\text{eff}} - y'_e = (4\pi/9)\beta\rho(m')^2, \tag{90}$$

where the Clausius-Mossotti equation can be used in place of y'_e. Also, y_{ind} can be replaced with y'_e for many practical calculations. The dipole moment m' is typically higher than the gas-phase dipole m (m' as high as 3.09 D vs $m = 1.83$ D was reported for water[86]) and needs to be either determined from experiment or estimated from calculations. The Wertheim theory of polarizable liquids[82] provides an analytic route for m' consistent with simulations of dipolar liquids without specific interactions.[31]

VI. Discussion

The separation of the solvent polarization into the slow nuclear and fast electronic components in application to problems related to electron mobility in polarizable media was considered by Pekar 70 years ago.[3] Within dielectric continuum models, this separation leads to the appearance in the factor c_0, the Pekar factor, in the nuclear solvation free energies. The main qualitative result is a significant drop (by about a factor of two for a typical value $\epsilon_\infty \simeq 2$) of the nuclear solvation free energy compared to its total (electronic plus nuclear) magnitude in a polar solvent with $\epsilon_s \gg 1$ (Figs. 2 and 3). Here, we have studied the separation into the fast and slow polarization in molecular liquids without relying on the continuum approximation. Our conclusions are threefold: (i) we confirm that the Pekar factor yields numerically reliable longitudinal solvation susceptibility when the continuum limit is taken in the microscopic susceptibility functions (Fig. 2), (ii) the functionality for the continuum longitudinal susceptibility following from the microscopic theories is distinct from the Pekar factor (Eq. (8)), and (iii) we find that the combination of continuum electrostatics with the Pekar factor yields a too strong decrease of λ with increasing ϵ_∞. A nearly constant λ (polarizable dipolar fluids, Fig. 3) or an increasing one (polarizable water, Fig. 4) are found from our illustrative calculations.

The first step of our analysis was to construct the nuclear solvation susceptibility by eliminating the fast component from the free energy functional. Our approach here follows the Marcus prescription.[23] However, we do not apply any specific assumptions regarding the electronic susceptibility of the bulk solvent or a specific form of the electronic-nuclear cross term in the functional. Both are left to be determined from numerical simulations. The macroscopic limit is then taken by extrapolating the results of simulation to $k = 0$. The resulting nuclear susceptibilities [Eq. (57)] appear as a combination of the susceptibility χ_{nn}^L, describing the variance of the nuclear polarization in the bulk liquid, and the screening function q^L, describing the screening of the external field by the induced dipoles. The latter parameter turns out to be consistent with the mean-field calculations producing the Clausius-Mossotti limit for ϵ_∞ [Eq. (42)]. As discussed above, there is generally no single continuum limit for a given solvent model since a whole family of mean-field continua can be constructed based on the scaling parameter Θ introduced by Høye and Stell.[21] Our simulations confirm that $\Theta = 0$ is consistent with the statistics of dense dipolar-polarizable fluids.

In is important to stress the distinction between our analysis and the studies of the relative performance of polarizable and non-polarizable force fields of the solvent used in numerical simulations.[87] Such force fields are parametrized to reproduce the same set of macroscopic properties of a given liquid. For instance, for water models, polarizable and non-polarizable force fields carry different permanent dipoles to fit the dielectric properties of ambient water. In contrast, the permanent dipole of the solvent molecules is kept constant in our analysis, which also implies that the dielectric constant and the effective condensed-phase dipole moment increase with increasing ϵ_∞ (see Table S1 and Fig. S7 in supplementary material[69]). Our observation that the reorganization energy in a given dipolar liquid is nearly constant as a function of ϵ_∞ implies that simulation results require very minor correction for the polarizability effects. At the same time, an enhanced effective dipole in the force field can potentially lead to an overestimate of λ by simulations. In the case of water, showing an increasing $\lambda(\epsilon_\infty)$ (open circles in Fig. 4), a non-polarizable force field with an enhanced permanent dipole can potentially reproduce the results in a polarizable force field.

Our study has focused on the goal of arriving at the continuum limit from finite-size numerical simulations

and on the task of testing the microscopic relevance of the Pekar factor. We have therefore neglected several issues important for specific microscopic calculations of solvation free energies and energetics of electron-transfer reactions. First, we neglected the transverse polar response in our calculations of the reorganization energy. This approach is justified in this setting since the entire foundation of the Marcus formula and the Pekar factor is based on limiting the theory to the longitudinal response (zero transverse response). We made an additional, and more drastic, approximation of neglecting the perturbation of the local density of the liquid induced by the repulsive core of the solute.[59] This component disappears from the reorganization energy in the continuum limit neglecting the solvent granularity, $\sigma \to 0$, which is achieved by increasing the solute/solvent size ratio. This approximation is, therefore, fully justified for the calculation of the continuum nuclear susceptibility χ_m^L shown in Fig. 2. However, our specific calculations of the reorganization energy shown in Figs. 3, 4, and 9 lack that density reorganization.[84] The relative values of the Marcus and microscopic reorganization energies are therefore subject to this uncertainty and should be viewed as illustrations to support the general statements made in the paper. The microscopic reorganization energy typically shifts upward by 20-30% when its density component is taken into account.[83]

The Pekar partitioning of the longitudinal response of the polarized medium to an external field was echoed by the theories of McRae and Lippert applied to spectral shift of optical dyes modeled as point dipoles altered by optical transitions.[88–90] In that case the partitioning was applied to the Onsager formula for dipole solvation involving a non-trivial combination of the longitudinal and transverse susceptibilities [Eq. (26)]. The assumption of additivity of interfacial polarization, implicit to this scheme, was criticized by Brady and Carr[17] and by other authors.[91] The resolution of the problem suggested by Brady and Carr[17] was to shift additivity from the solvation response to the dielectric transverse susceptibility of the bulk[92] $\chi^T = \chi_e^T + \chi_n^T$. According to their recipe, adopted in a number of publications,[30,49,91] the nuclear solvation response can be found by multiplying the total solvation response with the ratio χ_n^T/χ^T.

The idea of additivity of the transverse susceptibility is, however, as much a misconception as that of additivity of the interfacial polarization. The transverse susceptibility of bulk dielectric measured in the standard dielectric experiment is the $k \to 0$ limit of $\chi^T(k)$

$$\chi^T = \frac{\epsilon_s - 1}{4\pi} = \frac{\beta}{\Omega} \lim_{\mathbf{k}\to 0} \langle |\tilde{\mathbf{P}}_e^T + \tilde{\mathbf{P}}_n^T|^2 \rangle. \qquad (91)$$

A similar equation holds for the longitudinal susceptibility

$$\chi^L = \frac{\epsilon_s - 1}{4\pi\epsilon_s} = \frac{\beta}{\Omega} \lim_{\mathbf{k}\to 0} \langle |\tilde{\mathbf{P}}_e^L + \tilde{\mathbf{P}}_n^L|^2 \rangle. \qquad (92)$$

Each of the variances, $\langle |\tilde{\mathbf{P}}^L|^2 \rangle$ and $\langle |\mathbf{P}^T|^2 \rangle$, includes a long-range component, making the result dependent on the shape of the sample.[29,77] This component is eliminated in the trace $\chi^L + 2\chi^T$, leading to the Kirkwood-Onsager equation [Eq. (27)], which is independent of the sample shape.[28,93]

The variance of the transverse dipole ($\tilde{\mathbf{P}}^T \to \mathbf{M}^T$ at $k \to 0$) obviously includes the self components of the induced and permanent dipole and the cross term. However, the cross correlations relax on the time-scale of the nuclear dipoles and are therefore combined with $\langle |\mathbf{P}_n^\gamma|^2 \rangle$ in terms of the effective condensed-phase molecular dipole.[27,28] This prescription, which results in the standard empirical separation between low-frequency and high-frequency dielectric susceptibilities in the dielectric experiment,[9] is only possible because the nuclear dipoles are in equilibrium at high frequencies and the entire cross-correlation effect can be absorbed into the effective condensed-phase dipole [Eq. (90)]. If the nuclear polarization is brought out of equilibrium, as required for the non-equilibrium functional, the cross correlations have to be accounted for explicitly.

These arguments are brought up here to stress that the issues which make partitioning into the fast and slow polarization modes difficult in solvation problems are all present already for the dielectric response of a homogeneous polar liquid. The Brady and Carr scheme in fact employs the Pekar partitioning for the homogeneous liquid in order to justify a new, non-Pekar partitioning for the solvation problem. This conceptually inconsistent approach is not needed, as we have shown here. We start with the Marcus partitioning for the electronic and nuclear susceptibilities of bulk solvent to show that the ultimate result for the nuclear (longitudinal) solvation susceptibility is numerically consistent with the Pekar factor (Fig. 2). While we reach this result here from consistently microscopic models of the polar liquid, the same outcome follows from mean-field considerations.[61] In order to achieve this final result, cross correlations between induced and permanent dipoles need to be consistently taken into account. We still want to note that from the practical perspective, the Brady and Carr partitioning significantly reduces the dependence of the nuclear solvent response on the solvent polarizability,[18,91] in qualitative agreement with our results. However, from our calculations, this reduced dependence on the medium polarizability does not occur in the continuum limit, where typical PCM calculations operate.[49] The reduction, as shown in Figs. 3 and 4, occurs only in microscopic calculations, when the full nonlocal susceptibility function is employed, instead of its $k = 0$ value entering the dielectric calculations.

VII. Summary

We have taken a fresh look at the old problem of separating the polarization of a polar liquid into fast electronic and slow nuclear components. The theory for nuclear solvation susceptibility is formulated in terms of a 2×2 matrix of nonlocal, reciprocal-space susceptibility functions produced by numerical simulations. We arrive

at the continuum limit from the bottom up, by extrapolating the computed susceptibility functions to $k \to 0$. The Pekar factor turns out to yield a numerically reliable continuum longitudinal susceptibility. Nevertheless, a distinctly different functionality is produced from the microscopic theories. Illustrative calculations show a much weaker dependence of the nuclear solvation free energy on the polarizability of the solvent compared to the continuum Pekar prediction. Calculations presented here are limited to the longitudinal response. More complex solute configurations, including the Onsager limit of a spherical point dipole, require a separate consideration.

Supplementary material

See supplementary material for the simulation protocols, data analysis, and the derivation of Eqs. (45) and (50).

Acknowledgments

This research was supported by the Office of Basic Energy Sciences, Division of Chemical Sciences, Geosciences, and Energy Biosciences, Department of Energy (DE-SC0015641). CPU time was provided by the National Science Foundation through XSEDE resources (TG-MCB080071).

[1] P. W. Anderson, in *Solid State Physics*, Vol. 14, edited by F. Seitz and D. Turnbull (Academic Press, New York, 1963) pp. 99–214.
[2] L. D. Landau, Phys. Z. Sowiet. **3**, 664, 1933, in *Collected papers of L. D. Landau*, edited by D. T. Haar (Gordon and Breach, New York, 1965).
[3] S. I. Pekar, JETPh **16**, 341 (1946).
[4] R. P. Feynman, Phys. Rev. **97**, 660 (1955).
[5] R. Zwanzig, J. Chem. Phys. **38**, 1603 (1963).
[6] J. Hubbard and L. Onsager, J. Chem. Phys. **67**, 4850 (1977).
[7] H. Fröhlich, *Theory of dielectrics* (Oxford University Press, Oxford, 1958).
[8] B. K. P. Scaife, *Principles of dielectrics* (Clarendon Press, Oxford, 1998).
[9] C. J. F. Böttcher, *Theory of Electric Polarization*, Vol. 1 (Elsevier, Amsterdam, 1973).
[10] S. I. Pekar, *Research in electron theory of crystals* (USAEC, Washington, D.C., 1963).
[11] R. A. Marcus and N. Sutin, Biochim. Biophys. Acta **811**, 265 (1985).
[12] A. Nitzan, *Chemical Dynamics in Condensed Phases: Relaxation, Transfer and Reactions in Condensed Molecular Systems* (Oxford University Press, Oxford, 2006).
[13] P. F. Barbara, T. J. Meyer, and M. A. Ratner, J. Phys. Chem. **100**, 13148 (1996).
[14] M. D. Newton, Coord. Chem. Rev. **238–239**, 167 (2003).
[15] L. Reynolds, J. A. Gardecki, S. J. V. Frankland, and M. Maroncelli, J. Phys. Chem. **100**, 10337 (1996).
[16] D. V. Matyushov and M. D. Newton, J. Phys. Chem. A **105**, 8516 (2001).
[17] J. E. Brady and P. W. Carr, J. Phys. Chem. **89**, 5759 (1985).
[18] M. A. Aguilar, J. Phys. Chem. A **105**, 10393 (2001).
[19] M. D. Newton and H. L. Friedman, J. Chem. Phys. **88**, 4460 (1988).
[20] D. Kivelson and H. Friedman, J. Phys. Chem. **93**, 7026 (1989).
[21] J. S. Høye and G. Stell, J. Chem. Phys. **64**, 1952 (1976).
[22] R. Kubo, Rep. Prog. Phys. **29**, 255 (1966).
[23] R. A. Marcus, J. Chem. Phys. **24**, 979 (1956).
[24] B. U. Felderhof, J. Chem. Phys. **67**, 493 (1977).
[25] S. Lee and J. T. Hynes, J. Chem. Phys. **88**, 6853 (1988).
[26] B. U. Felderhof, J. Phys. C **12**, 2423 (1979).
[27] L. Onsager, J. Am. Chem. Soc. **58**, 1486 (1936).
[28] G. Stell, G. N. Patey, and J. S. Høye, Adv. Chem. Phys. **48**, 183 (1981).
[29] P. Madden and D. Kivelson, Adv. Chem. Phys. **56**, 467 (1984).
[30] M. Cossi and V. Barone, J. Phys. Chem. A **104**, 10614 (2000).
[31] S. Gupta and D. V. Matyushov, J. Phys. Chem. A **108**, 2087 (2004).
[32] A. A. Milischuk, D. V. Matyushov, and M. D. Newton, Chem. Phys. **324**, 172 (2006).
[33] R. A. Marcus, J. Chem. Phys. **24**, 966 (1956).
[34] D. Kivelson and H. Friedman, J. Phys. Chem. **93**, 7026 (1989).
[35] T. Fonseca and B. M. Ladanyi, J. Chem. Phys. **11**, 8148 (1990).
[36] F. O. Raineri, H. Resat, and H. L. Friedman, J. Chem. Phys. **96**, 3068 (1992).
[37] F. Raineri and H. Friedman, J. Chem. Phys. **98**, 8910 (1993).
[38] A. C. Maggs and R. Everaers, Phys. Rev. Lett. **96**, 230603 (2006).
[39] A. Chandra and B. Bagchi, J. Chem. Phys. **94**, 2258 (1991).
[40] R. A. Marcus, J. Phys. Chem. **98**, 7170 (1994).
[41] A. M. Kuznetsov and I. G. Medvedev, J. Phys. Chem. **100**, 5721 (1996).
[42] J. D. Jackson, *Classical Electrodynamics* (Wiley, New York, 1999).
[43] J. S. Høye and G. Stell, J. Chem. Phys. **72**, 1597 (1980).
[44] D. V. Matyushov, J. Chem. Phys. **140**, 224506 (2014).
[45] D. V. Matyushov, J. Chem. Phys. **120**, 1375 (2004).
[46] Y. I. Kharkats, A. A. Kornyshev, and M. A. Vorotyntsev, Faraday Trans. II **72**, 361 (1976).
[47] R. A. Marcus, Annu. Rev. Phys. Chem. **15**, 155 (1964).
[48] Y.-P. Liu and M. D. Newton, J. Phys. Chem. **98**, 7162 (1994).
[49] M. A. Aguilar, F. J. Olivares del Valle, and J. Tomasi, J. Chem. Phys. **98**, 7375 (1993).
[50] J. Li, C. J. Cramer, and D. G. Truhlar, Int. J. Quantum Chem. **77**, 264 (2000).
[51] H.-A. Yu and M. Karplus, J. Chem. Phys. **89**, 2366 (1988).
[52] H. J. Kim and J. T. Hynes, J. Chem. Phys. **96**, 5088 (1992).
[53] M. V. Basilevsky and G. E. Chudinov, Chem. Phys. **157**, 327 (1991).
[54] L. D. Landau and E. M. Lifshitz, *Electrodynamics of Continuous Media* (Pergamon, Oxford, 1984).
[55] A. V. Marenich, J. Ho, M. L. Coote, C. J. Cramer, and D. G. Truhlar, Phys. Chem. Chem. Phys. **16**, 15068 (2014).
[56] D. V. Matyushov and B. M. Ladanyi, J. Chem. Phys. **108**, 6362 (1998).
[57] M. J. Thompson, K. S. Schweizer, and D. Chandler, J. Chem. Phys. **76**, 1128 (1982).
[58] D. Chandler, K. S. Schweizer, and P. G. Wolynes, Phys. Rev. Lett. **49**, 1100 (1982).
[59] D. Chandler, Phys. Rev. E **48**, 2898 (1993).
[60] I. V. Leontyev and A. A. Stuchebrukhov, J. Chem. Phys. **141**, 014103 (2014).
[61] D. V. Matyushov, Chem. Phys. **174**, 199 (1993).
[62] M. S. Wertheim, J. Chem. Phys. **55**, 4291 (1971).
[63] J. Weeks, D. Chandler, and H. C. Andersen, J. Chem. Phys. **54**, 5237 (1971).
[64] J. P. Hansen and I. R. McDonald, *Theory of Simple Liquids* (Academic Press, Amsterdam, 2003).
[65] D. F. Calef and P. G. Wolynes, J. Chem. Phys. **78**, 470 (1983).
[66] C. G. Gray and K. E. Gubbins, *Theory of Molecular Liquids* (Clarendon Press, Oxford, 1984).
[67] G. Jeanmairet, N. Levy, M. Levesque, and D. Borgis, J. Phys.: Condens. Matter **28**, 244005 (2016).
[68] M. S. Skaf and B. M. Ladanyi, J. Chem. Phys. **102**, 6542 (1995).
[69] See supplementary material at [URL will be inserted by AIP] for details of calculations and experimental procedures.
[70] G. Lamoureux, E. Harder, I. V. Vorobyov, B. Roux, and A. D. MacKerell, Jr., Chem. Phys. Lett. **418**, 245 (2006).
[71] J. C. Phillips, R. Braun, W. Wang, J. Gumbart, E. Tajkhorshid, E. Villa, C. Chipot, R. D. Skeel, L. Kalé, and K. Schulten, J. Comput. Chem. **26**, 1781 (2005).
[72] M. S. Skaf, T. Fonseca, and B. M. Ladanyi, J. Chem. Phys. **98**, 8929 (1993).

[73] J. Cao and B. J. Berne, J. Chem. Phys. **99**, 6998 (1993).
[74] "MCPOL, http://theochemlab.asu.edu/?q=mcpol," (2016).
[75] F. J. Vesely, J. Comp. Phys. **24**, 361 (1976).
[76] M. P. Allen and D. J. Tildesley, *Computer Simulation of Liquids* (Clarendon Press, Oxford, 1996).
[77] M. Neumann, Mol. Phys. **57**, 97 (1986).
[78] G. Lamoureux and B. Roux, J. Chem. Phys. **119**, 3025 (2003).
[79] H. L. Friedman, *A Course in Statistical Mechanics* (Prentice-Hall, New Jersey, 1985).
[80] R. Schmid and D. V. Matyushov, J. Phys. Chem. **99**, 2393 (1995).
[81] A. V. Marenich, C. J. Cramer, D. G. Truhlar, C. A. Guido, B. Mennucci, G. Scalmani, and M. J. Frisch, Chem. Sci. **2**, 2143 (2011).
[82] M. S. Wertheim, Mol. Phys. **37**, 83 (1979).
[83] D. V. Matyushov, J. Chem. Phys. **120**, 7532 (2004).
[84] D. V. Matyushov, Mol. Phys. **79**, 795 (1993).
[85] The nonlocal susceptibilities adopted in Ref. 32 produce finctions $\chi_n^\gamma(k)$ very close to those reported here, except for the $k \to \infty$ asymptote which does not affect most practical calculations.
[86] M. Sharma, R. Resta, and R. Car, Phys. Rev. Lett. **98**, 247401 (2007).
[87] J. S. Bader, C. M. Cortis, and B. J. Berne, J. Chem. Phys. **106**, 2372 (1997).
[88] E. G. McRae, J. Phys. Chem. **61**, 562 (1957).
[89] E. Lippert, Z. Electrochem. **61**, 962 (1957).
[90] P. Suppan, J. Photochem. Photobiol. A **50** (1990).
[91] A. Klamt, J. Phys. Chem. **100** (1996).
[92] The additivity of transverse susceptibility comes from the empirical observation that the static dielectric constant can be represented as a sum of dielectric increments $\Delta\epsilon_j$ originating from separate relaxation processes with relaxation times τ_j.
[93] C. Zhang, J. Hutter, and M. Sprik, J. Phys. Chem. Lett. **7**, 2696 (2016).

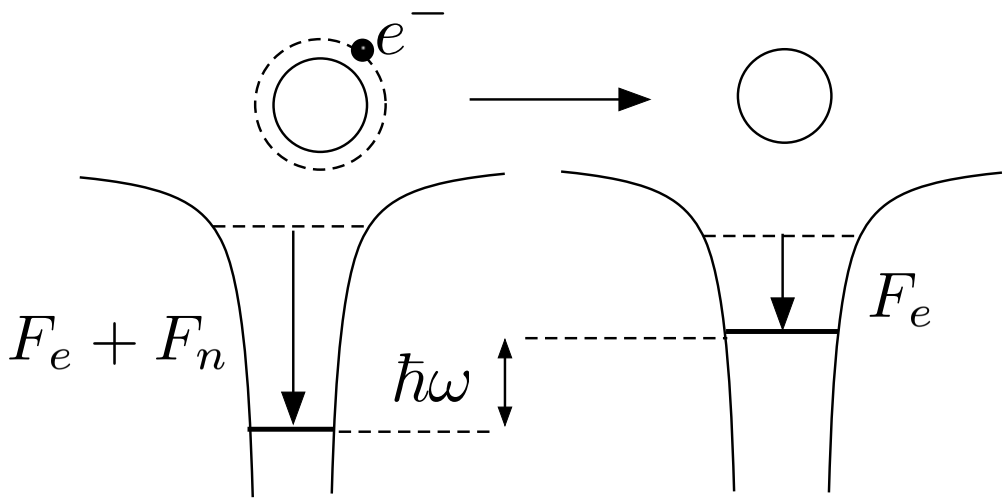
e^-
$F_e + F_n$
$\hbar\omega$
F_e

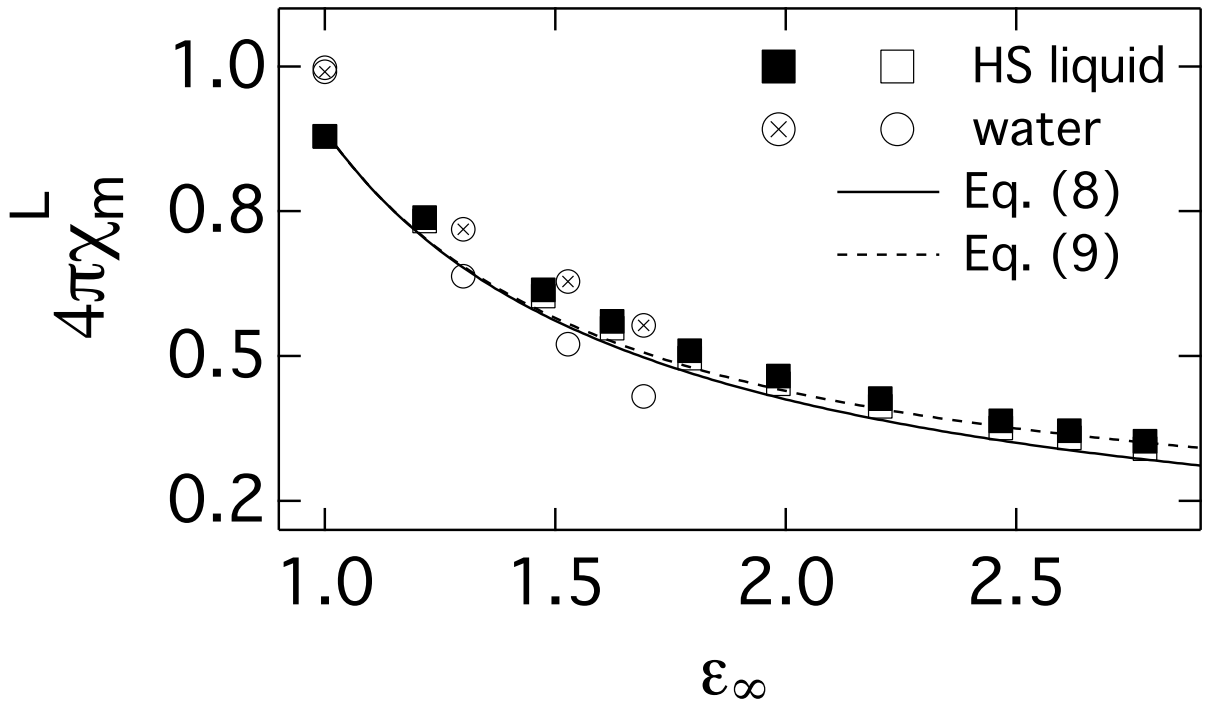
1.0
0.8
0.5
0.2
1.0
1.5
2.0
2.5
$\frac{L}{4\pi\chi_m}$
ε_∞
HS liquid
water
Eq. (8)
Eq. (9)

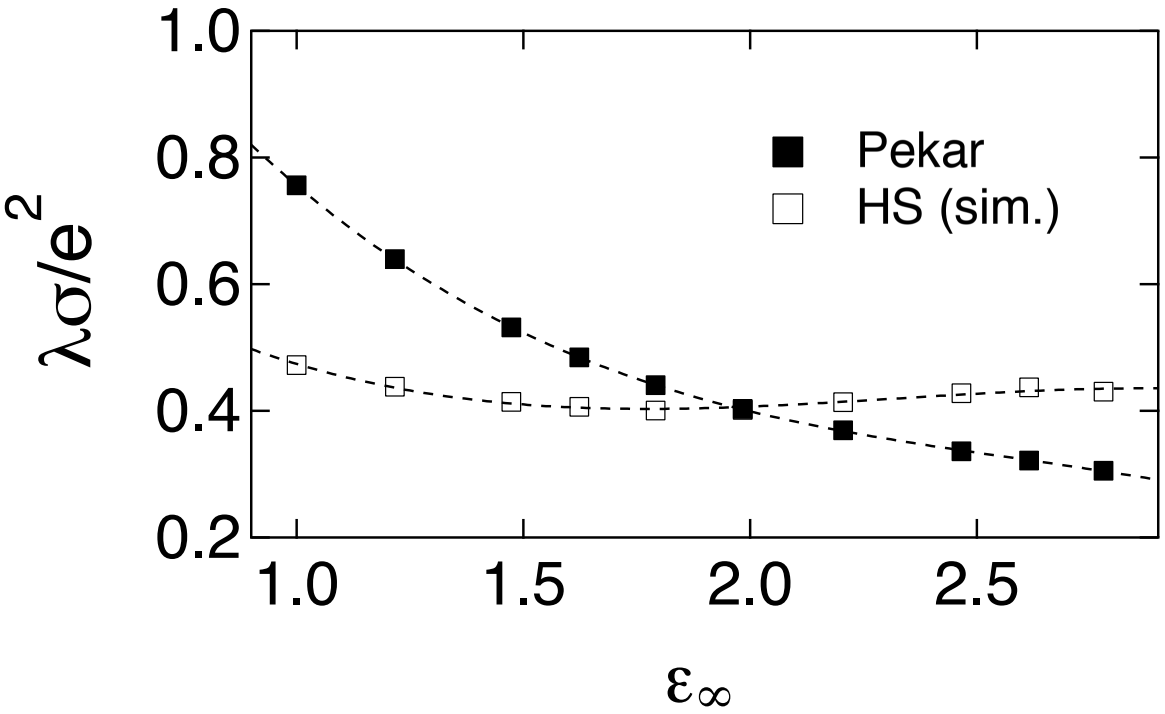
1.0
0.8
0.6
0.4
0.2
1.0
1.5
2.0
2.5
λσ/e²
ε∞
Pekar
HS (sim.)

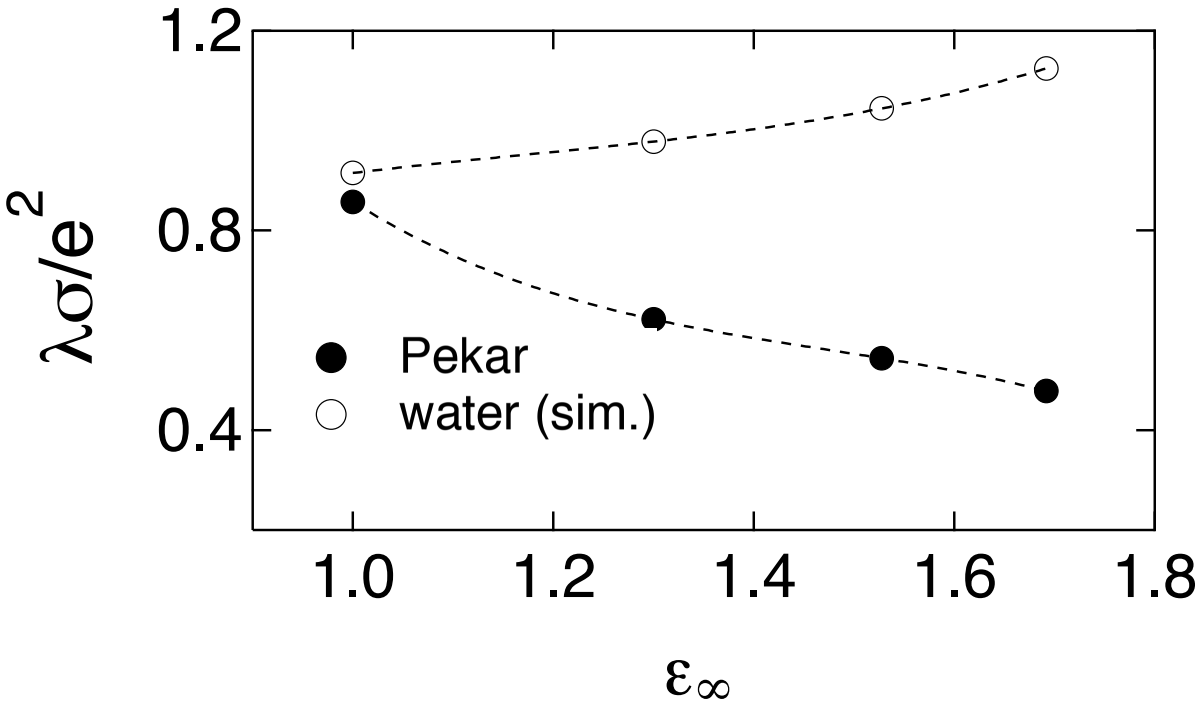
1.2
0.8
0.4
λσ/e²
Pekar
water (sim.)
1.0
1.2
1.4
1.6
1.8
ε∞

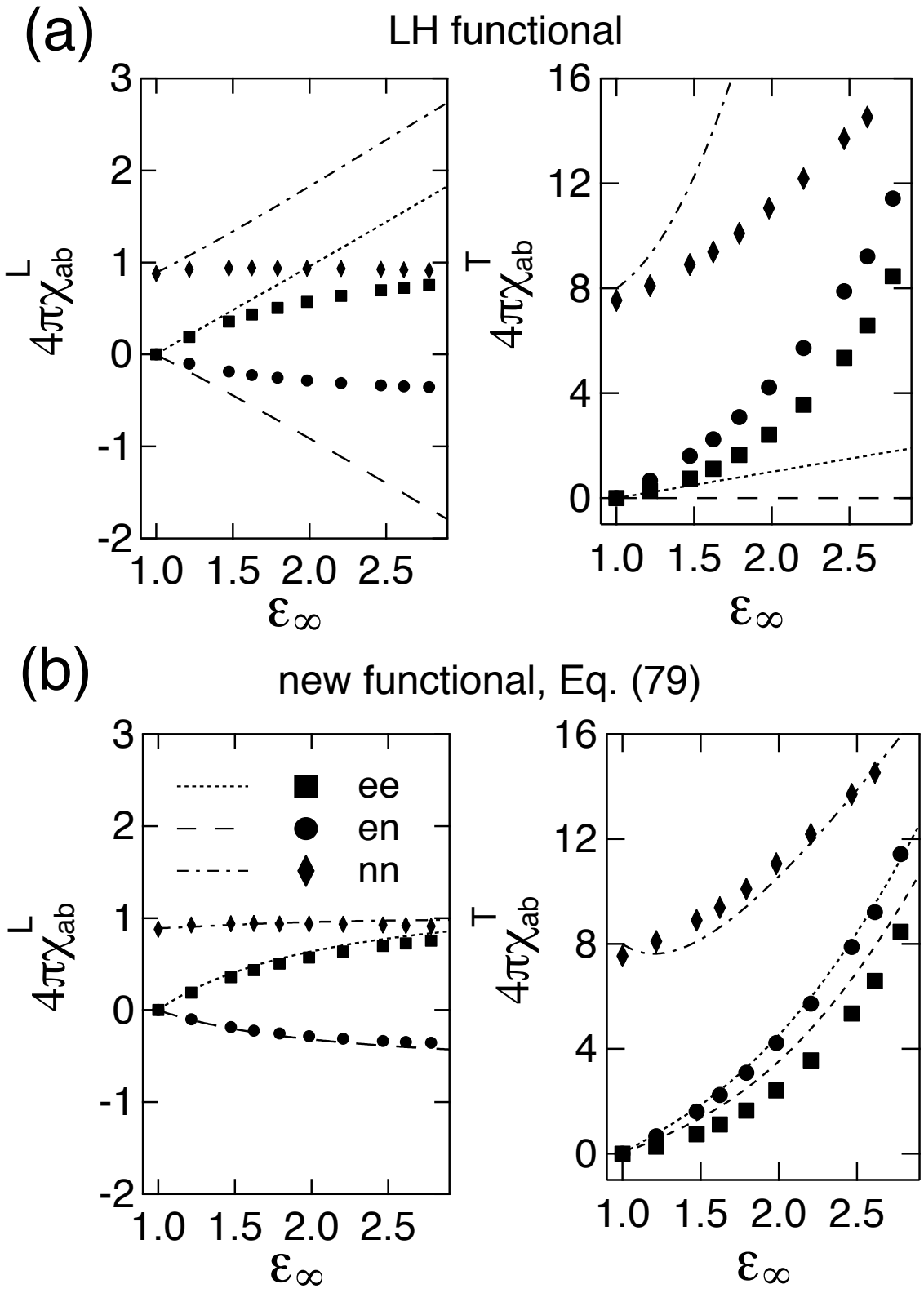
(a)
LH functional
$4\pi\chi_{ab}^{L}$
$4\pi\chi_{ab}^{T}$
ε_∞
(b)
new functional, Eq. (79)
ee
en
nn

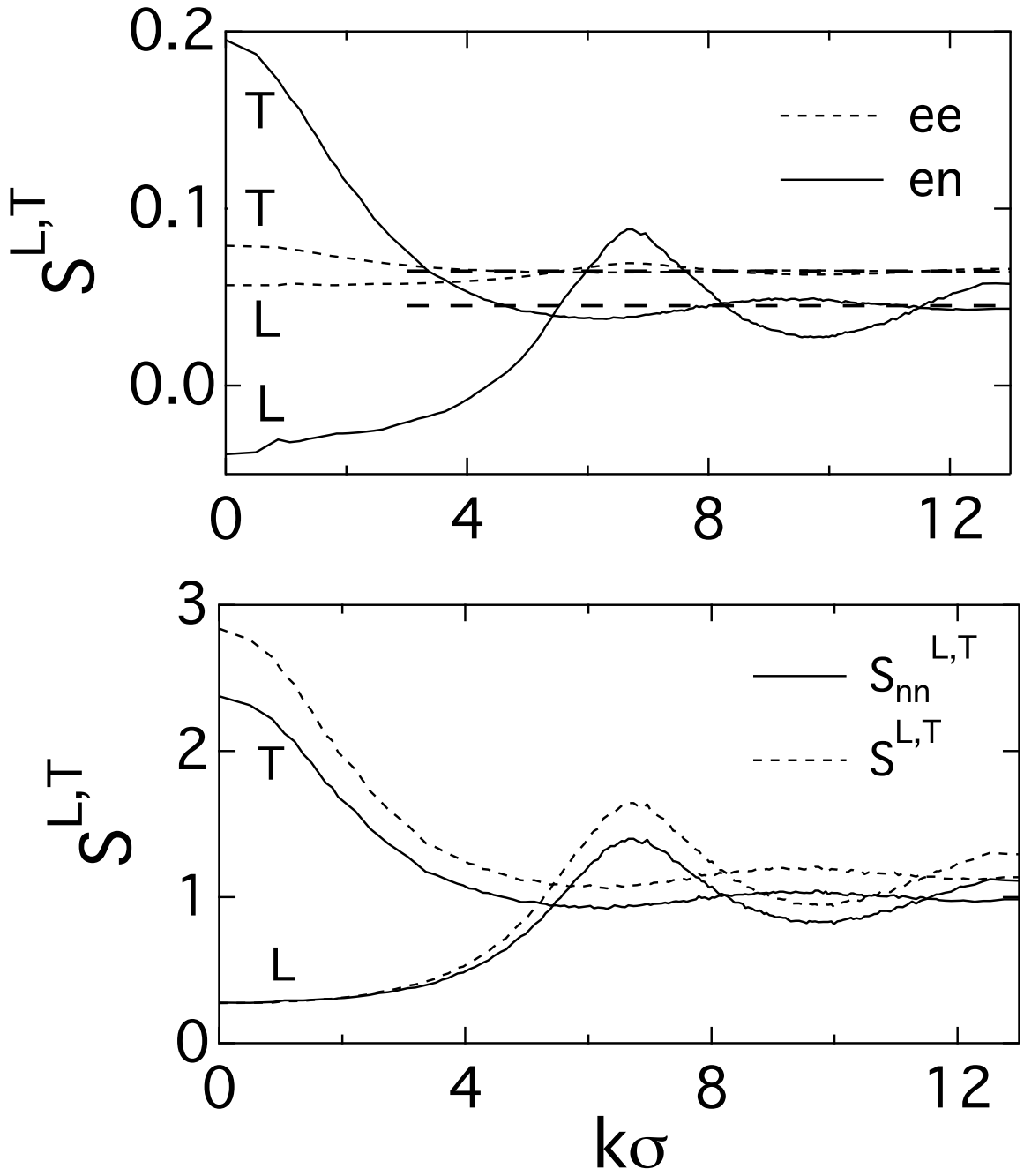
0.2
0.1
0.0
$S^{L,T}$
T
T
L
L
ee
en
0
4
8
12
3
2
1
0
$S^{L,T}$
T
L
$S_{nn}^{L,T}$
$s^{L,T}$
0
4
8
12
kσ

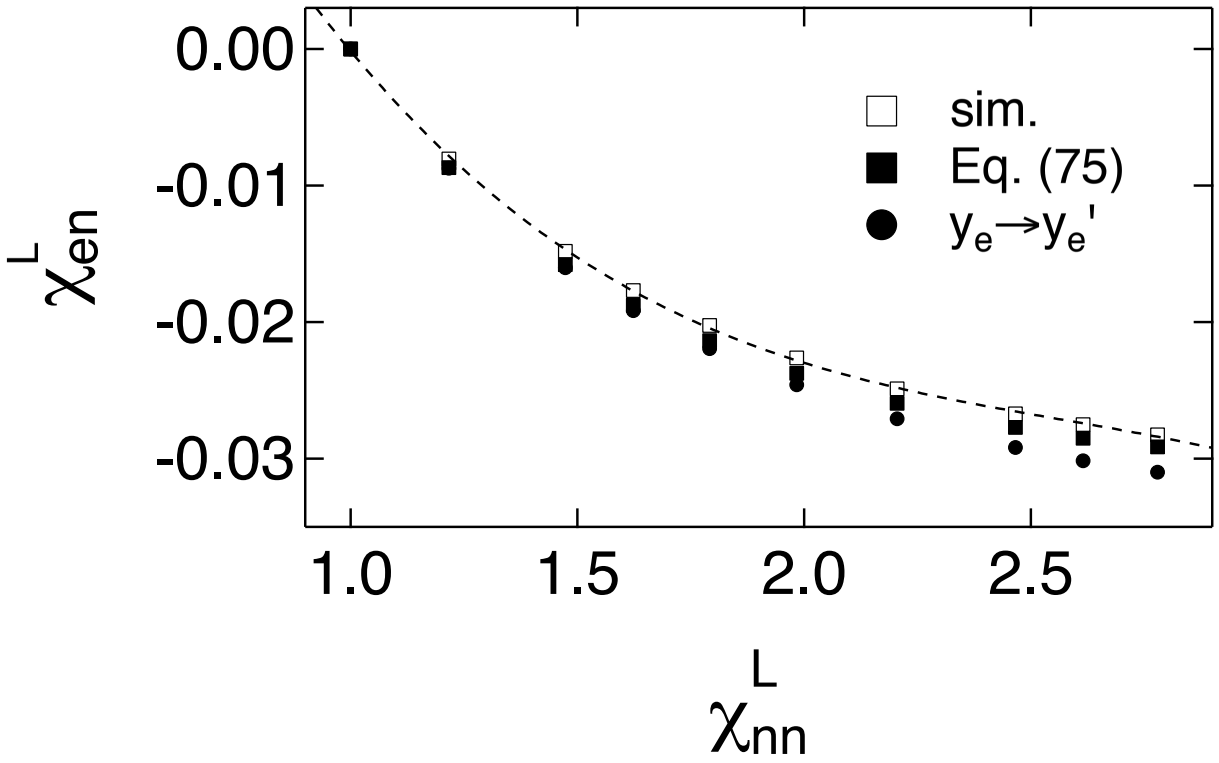
0.00
-0.01
-0.02
-0.03
1.0
1.5
2.0
2.5
sim.
Eq. (75)
$y_e \rightarrow y_e'$
χ_{en}^{L}
χ_{nn}^{L}

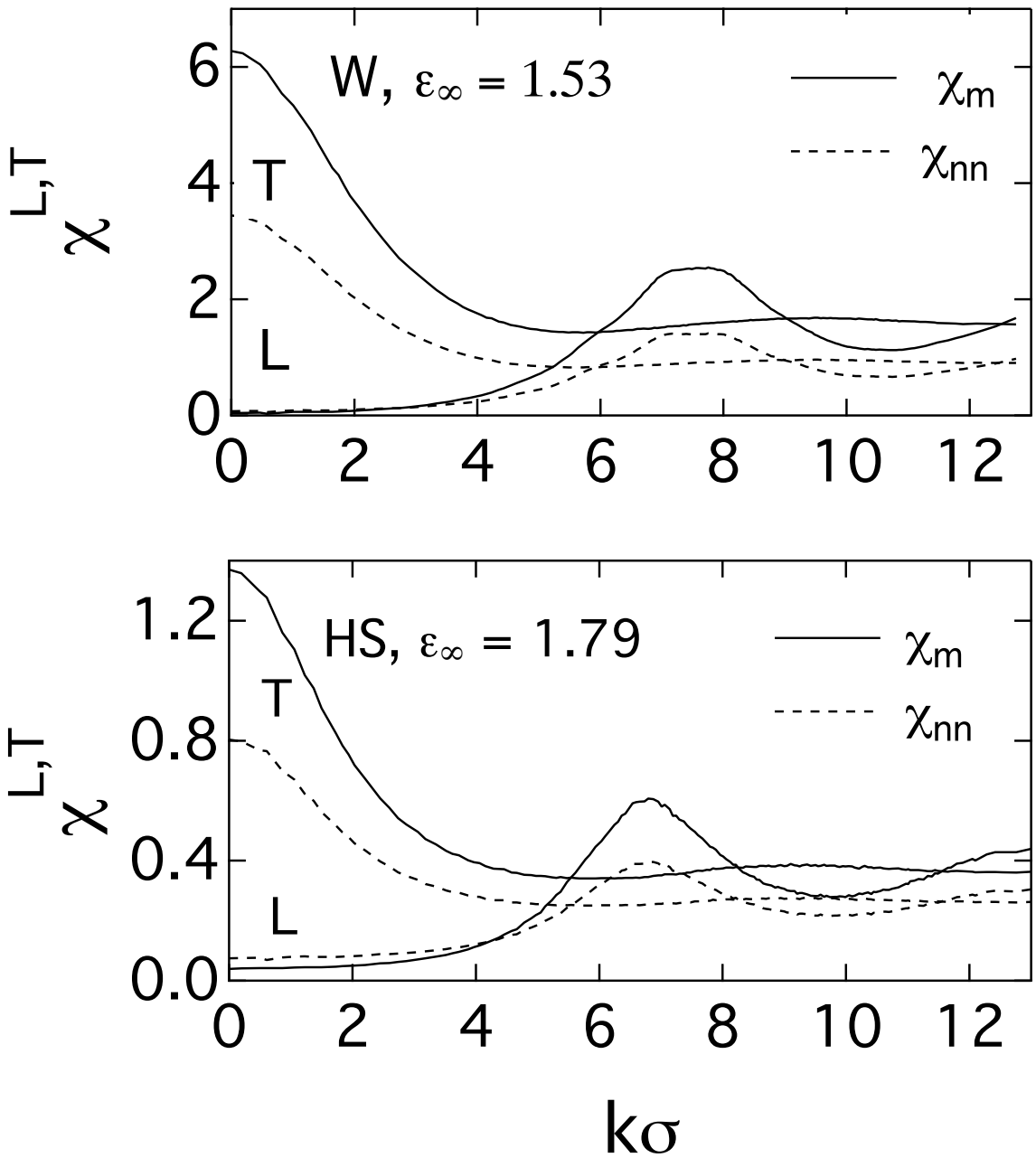
W, ε∞ = 1.53
χm
χnn
T
L
L,T
χ
HS, ε∞ = 1.79
kσ

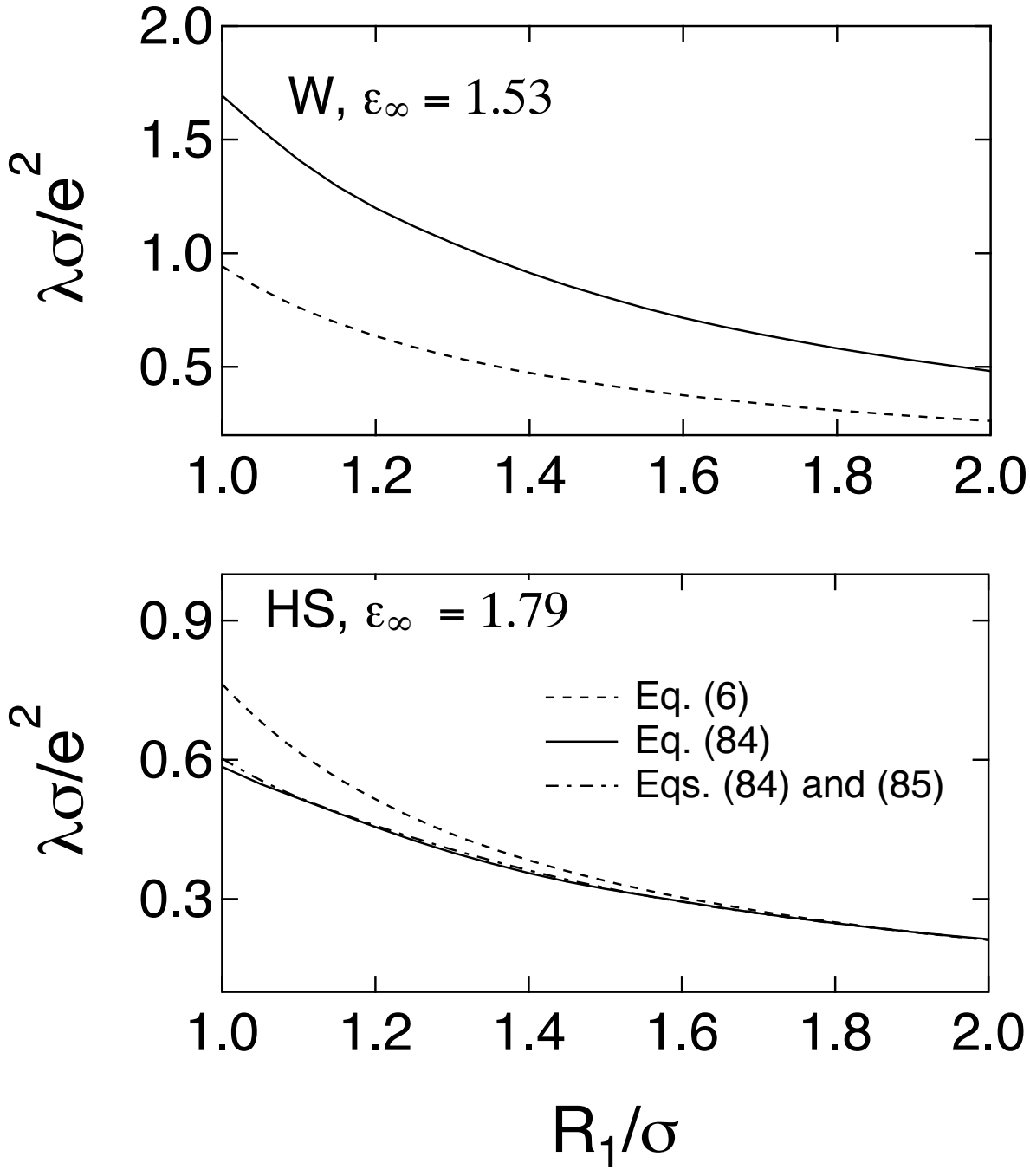
W, ε_∞ = 1.53
HS, ε_∞ = 1.79
Eq. (6)
Eq. (84)
Eqs. (84) and (85)
$\lambda\sigma/e^2$
R_1/σ
2.0
1.5
1.0
0.5
0.9
0.6
0.3
1.0
1.2
1.4
1.6
1.8
2.0

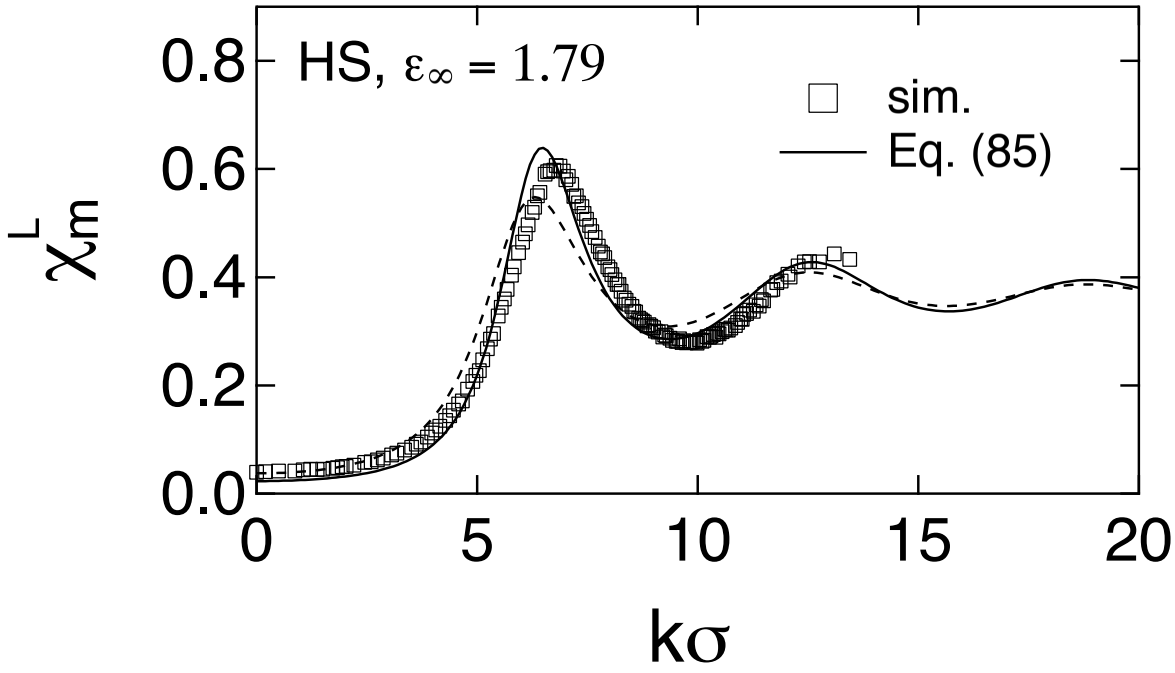
HS, $\varepsilon_\infty = 1.79$
sim.
Eq. (85)
χ_m^L
0.0
0.2
0.4
0.6
0.8
0
5
10
15
20
$k\sigma$

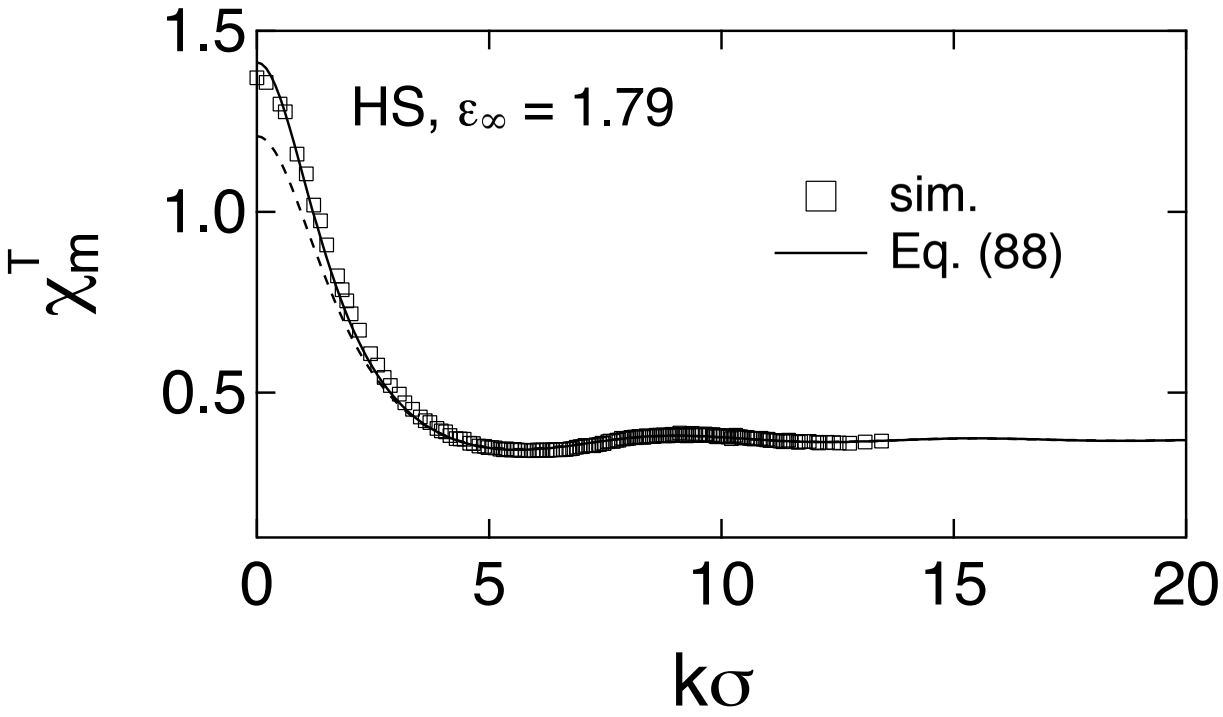
1.5
1.0
0.5
0
5
10
15
20
HS, ε∞ = 1.79
sim.
Eq. (88)
T
χm
kσ